PCCP

ROYAL SOCIETY OF CHEMISTRY

PERSPECTIVE

Cite this: *Phys. Chem. Chem. Phys.*, 2020, **22**, 11174

High-throughput experimentation meets artificial intelligence: a new pathway to catalyst discovery

Katherine McCullough, Travis Williams, Kathleen Mingle, Pooyan Jamshidi and Jochen Lauterbach *

Received 21st February 2020,
Accepted 30th April 2020

DOI: 10.1039/d0cp00972e

rsc.li/pccp

High throughput experimentation in heterogeneous catalysis provides an efficient solution to the generation of large datasets under reproducible conditions. Knowledge extraction from these datasets has mostly been performed using statistical methods, targeting the optimization of catalyst formulations. The combination of advanced machine learning methodologies with high-throughput experimentation has enormous potential to accelerate the predictive discovery of novel catalyst formulations that do not exist with current statistical design of experiments. This perspective describes selective examples ranging from statistical design of experiments for catalyst synthesis to genetic algorithms applied to catalyst optimization, and finally random forest machine learning using experimental data for the discovery of novel catalysts. Lastly, this perspective also provides an outlook on advanced machine learning methodologies as applied to experimental data for materials discovery.

Introduction

In "ancient" times (*i.e.*, a few decades ago), materials discovery was predominantly conducted *via* single trial-and-error experiments guided by human intuition and previous knowledge. Some classical examples of this research approach include material discovery conducted by Thomas Edison, who screened roughly 6000 materials for the filament of incandescent light bulbs.[1] Another example is the catalyst development work performed in the early 20th century by Mittasch and coworkers, who screened over 2500 compositions for the optimum ammonia synthesis catalyst.[2] However, this trial-and-error approach to materials discovery and optimization suffers from the time-consuming sequential nature of synthesis, analysis, and testing of materials for their desired properties. In addition, the process is costly and can result in wasting a lot of materials due to the trial and error nature of the process.

The concept of gradient libraries and systematic parallel screening for desired materials properties to accelerate materials discovery was introduced by the pioneering work of Hanak[3] in the 1970s. Over the following two decades, the methodology was adopted by several academic labs and companies. In 1986, for example, Creer *et al.*, designed and published a parallel catalyst screening system consisting of six parallel reactors attached to a gas chromatograph.[4] A comprehensive historical review on the early years of high throughput experimentation has been recently addressed by Maier.[5] Since those early beginnings, high throughput (HT) technologies have blossomed and have become routine in a variety of materials research fields, such as homogeneous and biocatalysis,[6–11] optical materials,[12,13] engineered biomaterials,[14] polymer-based materials,[15–17] and high entropy alloys.[18,19] The parallel screening, material discovery, and final optimization stages of the high throughput approach can be enhanced through several data science-based methods, which, when intelligently chosen, can extract intricate relationships between material synthesis variables (such as composition, synthesis parameters, *etc.*) and measurable material performance. The systematic mining of such relationships from multi-dimensional datasets that can be experimentally produced in a very efficient manner *via* high-throughput experimentation in conjunction with statistical methods for catalyst optimization can open new dimensions of catalyst research.

Machine learning (ML) has been recently employed in a variety of fields to significantly increase rates of discovery.[20,21] ML is a branch of artificial intelligence (AI) that employs statistical algorithms to identify important features in datasets and make predictions from these learned relationships between features and measured properties. Most ML algorithms currently reported in the literature are trained on computational data since many groups have amassed large databases. However, computational-based predictions do not always result in feasible materials formulations since experimental synthesis and application of the material incur additional complications not accounted for in the computational models.[22] Additionally, single low-throughput experimental methods do not generate enough data for ML to be truly useful. However, HT experimentation combined with ML can mitigate these drawbacks and will allow for the

College of Engineering and Computing, University of South Carolina, Columbia, SC 29208, USA. E-mail: lauteraj@cec.sc.edu

accurate prediction of stable and synthesizable materials. These algorithms have been used to identify phase boundaries in materials systems,[23] predict the formation of metallic glasses in ternary systems,[24] and accelerate electrocatalyst discovery.[25]

Experimentally trained ML models differ primarily with the amount of data accessible to the model. When large amounts of data are accessible (on the order of 10^4 or more data points), Deep Neural Networks (DNN) are typically adopted.[26] DNNs have been used in many applications with great success, including search engines,[27] playing board games against expert human players,[28] and clinical diagnoses.[29] DNNs are powerful, but they require a substantial amount of data for training to provide accurate predictions. When material systems contain small amounts of reported data (less than 10^3 data points), DNNs fail to produce accurate predictions. In this regime, many algorithms have been used and reported in the literature, including multiple regression,[30] least absolute shrinkage and selection operator (LASSO),[31,32] kernel ridge regression,[33] support vector machines,[34] neural networks,[35,36] and random forests.[37] Of these algorithms, the random forest (RF) model is consistently reported as having the highest accuracy for small and typically sparse experimental datasets.[38]

The combination of high throughput experiments with machine learning algorithms for characteristic determination of new materials is limited. Currently, high throughput methods are typically limited to be indirectly coupled with machine learning through the use of databases and material properties libraries. Materials can be synthesized rapidly through compositional spread alloys and thin films, and then their properties are determined and entered in databases. For heterogeneous catalysis, the additional complexity of operating conditions (*e.g.*, feed composition, space velocity, temperature) and catalyst preparation methods (*e.g.*, impregnation method, type of precursors, calcination parameters) leads to the need of more than just material properties for a machine learning training set. This complexity has led to very few studies coupling machine learning with experimental data in catalysis due to a large number of experiments that need to be run and the large number of variables to be considered. Here, we will discuss select examples of catalyst synthesis and optimization through statistical design of experiments (DoE), and then address the current state of machine learning coupled with high throughput experimentation. This is followed by an outlook on the future perspective of artificial intelligence coupled with experimental data, including the use of transfer learning from computational data to accelerate the discovery process.

High throughput screening methods for catalyst discovery

HT approaches are characterized not only by their throughput capabilities but also by their data quality and ability to adapt to different measurements. For heterogeneous catalysis, the additional complexity of measuring reaction temperatures, space velocities, catalytic activity, yield, and quantification of the product gases that often contain mixtures of similar species, presents a challenge for developing analytical systems that can acquire and analyze data in a rapid, parallel manner in order to determine quantitative structure–activity relationships. With the additional complexity of the effects of synthesis variables and operating conditions on catalyst performance across a variety of different reactions, multiple synthesis and screening methods have been developed that are suitable for the variety of applications. Bulk materials for catalytic studies are often synthesized in smaller sets of arrays (*i.e.*, tens to hundreds of samples) due to time-consuming multi-step synthesis methods that can involve mixing, heating, drying, milling, grinding and calcination steps that may be repeated multiple times. Combinatorial approaches to catalyst synthesis through solution-based methods have been demonstrated for perovskites,[39] molecular sieves,[40] colloidal nanoparticles[41] and near-infrared driven decomposition of solution-deposited films for the formation of mixed-metal electrocatalysts,[42] to name a few in the large body of work being developed in the field. High throughput experimentation can lead to the testing and discovery of more exotic materials than is permitted with the general one-at-a-time approach. However, without the aid of a researcher's domain knowledge in a particular reaction, the number of potential catalyst combinations for synthesis and experimentation is massive. A working understanding of the reaction chemistry, and hypothesis driven experimentation can dramatically reduce the possible catalyst combinations and lead to more intelligent design of experiments. This will have a strong impact on design space selection. Planning of the initial design space often requires implementation of DoE strategieses such as response surface methodologies and D optimal designs, of which have been thoroughly described elsewhere.[43,44] However the number of factors and parameters that can be screened is limited. Some of examples of intelligent selection of a design space for catalyst synthesis and experimentation either by implementing domain knowledge, DoE or a combination of both, will be highlighted in the case studies that follow.

Catalyst activity is often analyzed using parallel techniques to avoid the inefficient nature of sequential gas stream analysis through gas chromatography or mass spectrometry,[45,46] for example. However, in some instances these sequential techniques have been successfully applied to high throughput screening coupled with parallel reactors.[44,47–49] Parallel analysis of catalytic activity can be achieved using different optical imaging techniques, some of which may not provide chemical sensitivity or a linear dependence between the signal response and increase in catalytic activity.[44] In addition, imaging-based analysis techniques can be limited in their spatial resolution and thus their applicability depends greatly on the catalyst sampling density which in turn, is largely dependent on the method of synthesis and the reactor configuration. In order to determine structure activity relationships from HT experimental data, an appropriate method of analysis must be chosen that provides as much quantitative information as needed without sacrificing the amount of throughput that may be achieved.

Parallel analysis based on the cataluminescence (CTL) signal from solid catalyst surfaces under oxygen-containing environments has been demonstrated for small sets of catalysts.[50–54] The CTL response is created from the deactivation of intermediate species on the catalyst surface from the excited state to the ground state, thus producing light emission. This method of analysis however, is limited to a very small number of chemical reactions and multiple CTL sensing elements are needed for differing product species and identification. In contrast, the application of IR thermography (IRT)[55] has been highly effective for a larger range of array sizes spanning into the hundreds of samples, and for multiple reactions,[56–60] thus providing more flexibility than CTL. Catalytic activity is determined by IRT based on heats of reaction. This method is chemically insensitive and does not provide insight into competing parallel reaction pathways and cannot quantify catalyst selectivity. Thus, this method is often limited to reactions with single reaction pathways. Laser-induced fluorescence imaging (LIFI)[61–63] has also be utilized as an effective imaging technique for specific chemical reactants or products, where the intensity of the fluorescence of a specific molecule can be tuned and imaged with a charged coupled device. Spatially resolved Fourier transform infrared imaging (FTIR imaging) overcomes the drawback of IRT and CTL in terms of the chemical insensitivity and is useful for a broad range of chemistry. FTIR has been demonstrated for high-throughput screening of catalysts for a variety of reactions,[64–68] but typically with a lower throughput than can be achieved with IRT screening. A focal-plane array-based IR detector provides the spatial resolution needed for parallel analysis. Infrared spectroscopy is a useful technique due to its chemical sensitivity and ability to quantify reaction products due to the characteristically linear relationship between absorbance and concentration established through Beer's law. However, chemical speciation must be done with care and often requires chemometric approaches, as IR bands can become easily convoluted when multiple gases have similar vibrational modes. The use of IR imaging is most advantageous when each reaction product can be quantified with a unique IR band that does not have an overlap with another product.

With the ability to rapidly generate data using parallel screening and analysis techniques, data management methodologies must be utilized to avoid bottlenecking of the overall HT experimentation process. Additionally, proper data management leads to proper data analysis, and thus knowledge extraction of trends and quantifiable relationships.[44,69] Data mining tools used to extract knowledge can include principal component analysis (PCA), clustering techniques, genetic algorithms (GA), artificial neural networks (ANN), decision trees, and other classification and regression based machine learning algorithms.[44,70,71] The application of machine learning algorithms for data mining in catalysis will be discussed later on in greater detail.

The following examples were selected to showcase the use of different high-throughput experimentation techniques to either accelerate new material discovery or to elucidate qualitative structure–activity relationships. The examples represent a variety of studies. Many other outstanding studies have of course been published and can unfortunately not be discussed here.

Cu–Ag catalyzed ethylene epoxidation

The selective oxidation of ethylene to ethylene oxide (EO) is a highly profitable reaction occurring typically on α-Al_2O_3 supported promoted silver nanoparticles. The process was first commercialized by Union Carbide in 1937.[72,73] EO is used as an intermediary to form primarily ethylene glycols (antifreeze, polyester, PET), as well as polyethylene glycols (perfumes, cosmetics) and ethoxylates (detergents, surfactants, emulsifiers). In general, Ag is strong enough to dissociate oxygen and supply stable oxygen species for epoxidation, but not strong enough to break the ethylene C–H bond[74,75] making it the most effective catalyst for ethylene epoxidation. Cu is the only material predicted to have theoretical baseline ethylene oxide selectivity higher than Ag, but Cu epoxidation activity is hindered by the formation of surface Cu_2O.[76] A series of works from Barteau and coworkers demonstrated that Ag–Cu bimetallics have a synergistic effect on EO selectivity and conversion, and similar trends were observed in studies involving Ag–Cu bimetallic promoted by Cl and Cs. Kinetic studies for the Ag–Cu alloy indicated a reaction rate limited by the surface reaction of O and C=C under oxygen-rich conditions, and the dissociated of oxygen under ethylene rich conditions.[77] Additional promoting systems, which have been studied, include Ag/$SrTiO_3$ catalysts promoted with Au, Ba, Pd, Sn, and Cu. Here, it was found that only Au, Ba, and Cu improved the ethylene oxide selectivity relative to an Ag only catalyst.[78] While neither Pd or Sn improved selectivity or activity, the Sn–Cu–Ag system was effective in increasing the catalyst stability, presumably by decreasing coke formation. This result was similar to that of Bae *et al.*, who studied Sn promotion of the hydrochlorination of CCl_4 over Pt–Sn/γ-Al_2O_3 and found that Sn improved stability by destroying the Pt surface sites linked to coking and transferring electrons to Pt such that the HC–Pt bond strength lessened.[79] Work by Dellamorte *et al.* showed that 100 ppm Pd could potentially double the ethylene oxide selectivity when compared to a base silver catalyst, appearing to increase the rate of oxygen dissociation[80] while Chongterskool *et al.*[78] found that the addition of 0.63% Pd increased coking and ultimately decreased ethylene oxide selectivity. This may be due to the disparity in Pd loadings utilized.

Many of the promoting systems which have been studied for base Ag/α-Al_2O_3 catalysts have not systematically screened and optimized for incorporation into the bimetallic Cu–Ag/α-Al_2O_3 catalyst system. Here, as a first example of the interplay between HTE and statistical methods, we discuss a multi-tier optimization of the co-promoter space for Cu–Ag/α-Al_2O_3 catalyzed ethylene epoxidation *via* high-throughput reactor studies paired with the statistical DoE. First, novel promoting materials were screened with the objective of identifying systems that led to improved ethylene oxide selectivity on 0.2% Cu–15% Ag/α-Al_2O_3 based catalysts. Second, selected co-promoters were further studied using factorial designs to develop an understanding of how catalyst structure and promotional effects

change with respect to promoter loading and impregnation sequence. Finally, learnings were leveraged to incorporate the promoting materials into the base catalyst formulation.

Initial co-promoters were selected on the basis that they could either form stable alloys with Cu and/or Ag (*i.e.* Au, Ru, Zn, Pt, Mg, Pd) or had been shown in previous work, experimental or theoretical, to catalyze or promote epoxidation (*i.e.* Sn, Mo, Au, Pt, Cs, Pd, Re).[72,78–88] Each co-promoter was added to a 0.2% Cu–15% Ag/α-Al_2O_3 formulation as part of a standard wet impregnation synthesis[84] in the form of a water-soluble salt. Promoters were either co-impregnated on the support with Ag or sequentially impregnated onto the Ag-containing support after the Ag/α-Al_2O_3 had been dried, calcined and also reduced in a 20% hydrogen/helium stream at 300 °C for 12 h. X–Ag is used in catalyst nomenclature to denote a sequential impregnation preparation while (X–Ag) denotes co-impregnation, an example being (Cu–Sn)–Ag which means that Ag was impregnated, dried, and calcined before co-impregnating Cu and Sn in one step followed by an additional drying, calcination and final reduction before catalyst testing. Fig. 1 shows the co-promoters that were part of the initial screening as well as their corresponding loadings and the EO selectivity at 5 ± 0.5% C_2H_4 conversion for each of the co-promoted 0.2% Cu–15% Ag/α-Al_2O_3 catalysts. Measurements were made in 10% C_2H_4, 10% O_2, and balance N_2 feed at a space velocity of 4000 h^{-1} and at temperatures between 230–350 °C in order to achieve comparable conversion levels. Co-Promoters, which improved the ethylene oxide selectivity with respect to unpromoted Cu–Ag catalysts were selected for further investigation with factorial design, including Cs, Re, Au, and Sn. Previous studies focused on optimizing promoted alumina supported Cu–Ag and Ag catalysts showed sensitivity to the impregnation sequence and promoter loadings involved.[72,89] Thus, the parameters selected for continued investigation were the co-promoter impregnation order on the catalyst and the promoter loading. These parameters were studied using 2^2 factorial screening designs for each Cs, Re, Au, and Sn with the screening performed in our 16-well parallel reactor.[72,89]

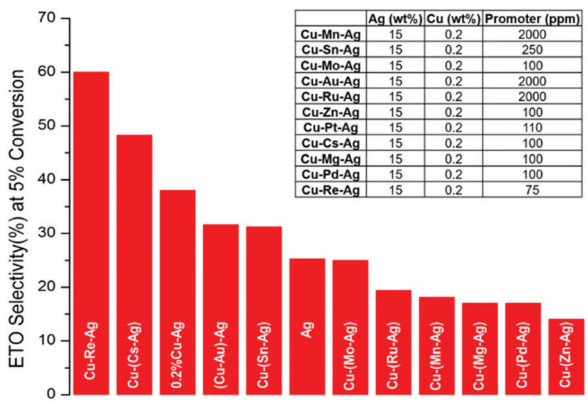

	Ag (wt%)	Cu (wt%)	Promoter (ppm)
Cu-Mn-Ag	15	0.2	2000
Cu-Sn-Ag	15	0.2	250
Cu-Mo-Ag	15	0.2	100
Cu-Au-Ag	15	0.2	2000
Cu-Ru-Ag	15	0.2	2000
Cu-Zn-Ag	15	0.2	100
Cu-Pt-Ag	15	0.2	110
Cu-Cs-Ag	15	0.2	100
Cu-Mg-Ag	15	0.2	100
Cu-Pd-Ag	15	0.2	100
Cu-Re-Ag	15	0.2	75

Fig. 1 Initial screening of co-promoters for ethylene epoxidation measured at differential conditions. Reaction conditions: 10% C_2H_4, 10% O_2, in balance N_2, SV = 4000 h^{-1}. The table inset shows the Ag, Cu and promoter weight loadings for each catalyst.

Interestingly, no statistically significant effects of these variables were found on the morphology or activity of Re and Au containing catalysts, but differences in Sn and Cs containing materials based on the levels studied were substantial. For example, the main effects of Cs loading and impregnation order for a Cs–0.2% Cu–15% Ag/α-Al_2O_3 catalyst on ethylene oxide selectivity at 5% C_2H_4 conversion demonstrated that selectivity increased with increasing Cs loading and decreased when Cs was co-impregnated with Cs rather than Ag. As a note, the design was centered around the original starting point in the investigation of Cs loading pertaining to a 0.2% Cu–(100 ppm Cs–15% Ag)/α-Al_2O_3 catalyst and that this formulation was ultimately found to be the optimal loading for enhanced ethylene oxide selectivity.

Examination of SEM images of the Cs containing Cu–Ag/α-Al_2O_3 provided some insights into the above-described relationships. Fig. 2 shows that the average size of the Ag particles increased substantially when Cs was co-impregnated with Cu. The average size of Ag particles when Cs was co-impregnated with Ag was within error the same for the two Cs loadings, being 18.9 ± 8.5 nm for (a) Cu–(50 ppm Cs–Ag) and 15.7 ± 0.8 nm for (b) Cu–(150 ppm Cs–Ag). When Cs was instead impregnated with Cu the average size increased substantially to 201 ± 37.2 nm for (c) (Cu–50 ppm Cs)–Ag and was much less when more Cs was co-impregnated with Cu for (d) (Cu–150 ppm Cs)–Ag with an average Ag particle size of 55.4 ± 3.7 nm.

In the case of Sn, lower Sn loadings benefited EO selectivity, while impregnation order made little difference. In addition, it was found that the 0.2% Cu 15% Ag at all Sn loadings and impregnation sequences investigated formed unexpected porous agglomerates which could possibly arise due to the effects of Sn on the mobility of Cu and Ag during catalyst formation. SEM images are included in Fig. 3.

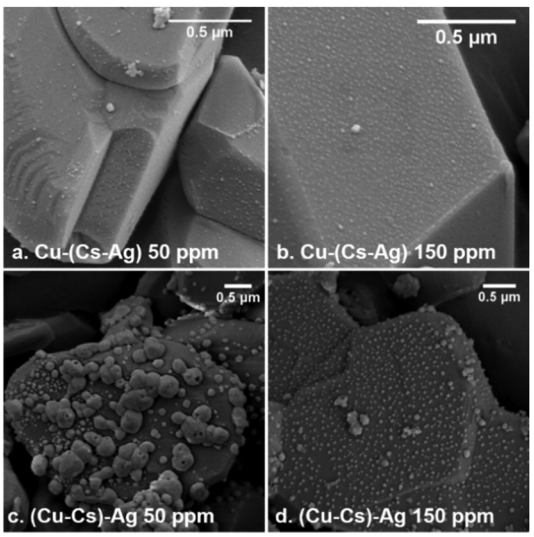

Fig. 2 SEM images of selected Cs promoted Cu–Ag/α-Al_2O_3 catalysts for ethylene epoxidation with varying synthesis impregnation methods, where the brackets signify the order the impregnation. (a) 0.2% Cu–(50 ppm Cs–15% Ag) (b) 0.2% Cu–(150 ppm Cs–15% Ag) (c) (0.2% Cu–50 ppm Cs)–15% Ag and (d) (0.2% Cu–150 ppm Cs)–15% Ag.

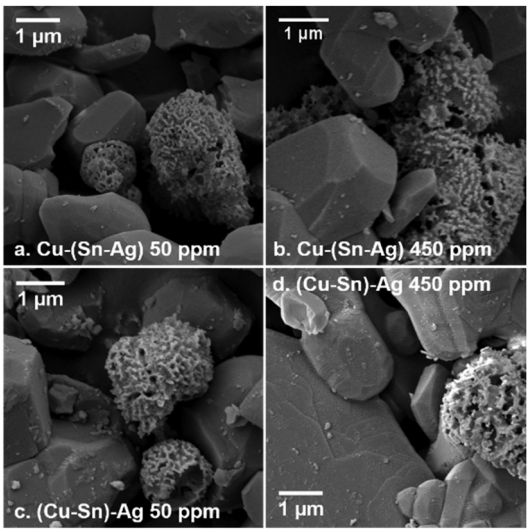

Fig. 3 SEM images of selected Sn promoted Cu–Ag/α-Al_2O_3 catalysts for ethylene epoxidation with varying synthesis impregnation methods, where the brackets signify the order the impregnation. (a) 0.2% Cu–(50 ppm Sn–15% Ag) (b) 0.2% Cu–(450 ppm Sn–15% Ag) (c) (0.2% Cu–50 ppm Sn)–15% Ag and (d) (0.2% Cu–450 ppm Sn)–15% Ag.

Using the optimized co-promoter (Sn, Cs, Re, Au) loadings and impregnation sequences, an optimized, fully promoted (Cu–Au)–Re–(Sn–Cs–Ag) catalyst was synthesized and evaluated. Additional catalyst formulations, including Au–Re–(Sn–Cs–Ag), Cu–Re–(Cs–Ag), and Re–(Cs–Ag), were synthesized as well for comparison. It should be noted that the purpose of synthesizing and comparing the fully promoted material to one containing only Re–(Cs–Ag) and Cu–Re–(Cs–Ag) was to evaluate the efficacy of the more obscure promoting materials (Sn and Au) when compared to Re and Cs, which are well known and expected to have a synergistic effect on epoxide selectivity.

The results of this analysis are shown in Fig. 4, together with the performance of the Ag only and Cu–Ag only catalysts for reference. Under the reaction conditions studied here, the fully promoted (Cu–Au)–Re–(Sn–Cs–Ag) catalyst promoted EO selectivity to a greater extent than all other materials evaluated, having an EO selectivity of roughly 69% at 5% ethylene conversion. This value is more than double that of the Ag only baseline catalyst. An interesting observation was that the same catalyst was 30% less selective toward EO when Cu was omitted from the formulation altogether. Conversely, the addition of Cu to Re–(Cs–Ag) lowered the EO selectivity by approximately 10%, possibly disturbing the Re and Cs synergistic effect.

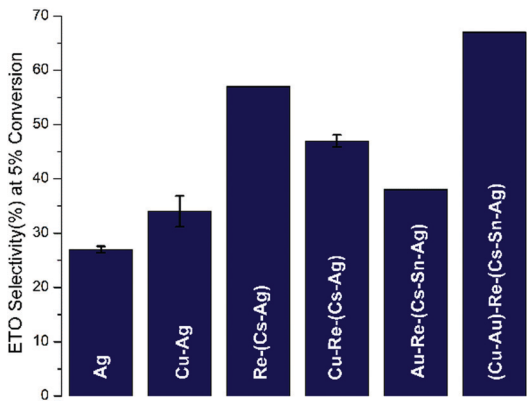

Fig. 4 Optimized co-promoter loadings and impregnation sequences for ethylene epoxidation on Ag/α-Al_2O_3 catalysts. Reaction conditions: 10% C_2H_4, 10% O_2, in balance N_2, SV = 4000 h^{-1}.

In summary, high-throughput analysis in combination with statistical DoE was used to complete a systematic screening of both conventional and nonconventional promoters for 0.2% Cu–15% Ag/α-Al_2O_3 ethylene epoxidation catalysts. The most promising candidates from the screening were found to be Au, Re, Sn, and Cs, each of which was optimized for the ideal impregnation sequence and loading. Results of the factorial analysis together with SEM studies led to the conclusion that increased Cs loading and co-impregnation with Ag were instrumental in decreasing the Ag particle size and increasing its dispersion on the α-Al_2O_3 support. In the case of Sn, it was found that lower Sn loadings benefited EO selectivity while the impregnation order made little difference. SEM studies showed that 0.2% Cu–15% Ag catalysts at all Sn loadings and impregnation sequences investigated displayed porous agglomerates which could arise due to the effects of Sn on the mobility of Cu and Ag. Knowledge gained through the study was used to direct the synthesis of a fully promoted (Cu–Au)–Re–(Sn–Cs–Ag)/α-Al_2O_3 catalyst, which was 69% selective toward ethylene epoxidation at 5% ethylene conversion, more than double that of the Ag only baseline catalyst evaluated at comparable conditions.

High throughput synthesis: PdBiTe catalysts for aerobic oxidative esterification of primary alcohols

Solution-based synthesis for bulk catalytic materials can be a primary bottleneck in the overall assessment of new material discovery *via* HT methodologies. Heterogeneous catalysts are often synthesized *via* incipient wetness impregnation, wet impregnation, hydro- or solvothermal treatment methods that require multiple steps and can take multiple days to complete.[90] Because of this, screening new heterogeneous catalysts can often be a gamble due to the lack of information available in the literature and the amount of time and cost required to synthesize many catalysts, especially if the purpose is for material discovery. To circumvent this issue, Mannel *et al.*[91] demonstrated a rapid synthesis method to screen a large number of materials for the aerobic oxidative esterification of primary alcohols by mimicking synthesis methods used for homogenous catalyst synthesis. Catalysts are prepared *in situ via* simple combination and mixing of different catalyst components, such as a metal salt and acid, base, or other additives. Certain heterogeneous catalyst compositions can be created in a similar matter, thus shortening steps involved in heterogeneous catalyst synthesis and preparation. Catalysts for aerobic oxidation of alcohols to aldehydes and ketones have been successfully identified in previous studies,[92,93] but analogs for the conversion of primary alcohols to carboxylic acids and

esters by homogenous catalysts have been less successful. Simple binary and ternary admixtures of Pd/charcoal (Pd/C) were combined with one or two metal and/or metalloid components as catalysts with no additional steps that are indicative of heterogeneous catalyst synthesis, such as calcination and reduction. This led to the screening of 400 different combinations for the oxidative methyl esterification of 1-octanol. After the initial screen, a response surface methodology was employed to further optimize the novel catalyst formulations.

Preliminary studies of the admixture screening had shown that the addition of $Bi(NO_3)_3$ and Te to a Pd/C is highly effective for the methyl esterification of a variety of primary alcohols. To further test the robustness of the admixture screening methodology, 28 different additives ranging from different main-group, transition metal, and rare earth elements were screened in either their oxide form, salt form, or in some cases both. These catalysts were tested for their aerobic oxidative methyl esterification activity of 1-octanol in methanol at 60 °C. In total 231 different elemental combinations and 406 unique admixtures were tested as catalysts for the reaction. The results from this screen are shown in Fig. 5.

The base catalyst of Pd/C exhibited a 32% yield for methyl octanoate and the addition of the variety of promoters to the catalyst ranged yields as low as 2% and as high as 88%. From this screening, it was found that Bi- or Pb-based additives, when combined with elemental Te, had the highest yield of methyl octanoate. Therefore, catalyst compositions of $PdBi_xTe_y/C$ were optimized using response surface methodology. A catalyst containing 1:1:1 molar ratio of PdBiTe was used as a starting point and four surrounding compositions were used to determine the gradient associated with the Bi and Te mole fractions. Two of the best catalysts discovered were $PdBi_{0.47}Te_{0.09}$ and $PdBi_{0.35}Te_{0.23}$. A response surface methodology was then enacted to further improve the activity and optimize a more precise heterogeneous catalyst formulation. One such combination, $PdBi_{0.35}Ti_{0.21}/C$ was shown to have excellent performance and good stability under continuous flow conditions in a packed bed reactor and is the most active liquid-phase oxidative esterification catalyst reported to date.

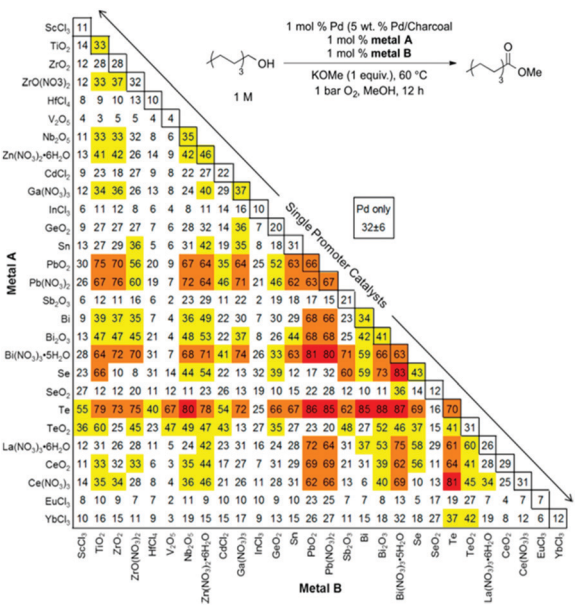

Fig. 5 Admixture screening data (methyl octanoate yields) obtained from the aerobic oxidation of 1-octanol with heterogeneous catalysts composed of Pd/C in combination with one or two additives. Color code reflects methyl octanoate yields below that obtained with Pd alone (white), above Pd alone (yellow), >60% (orange), and ≥80% (red). Adapted with permission from "Discovery of Multicomponent Heterogeneous Catalysts *via* Admixture Screening: PdBiTe Catalysts for Aerobic Oxidative Esterification of Primary Alcohol, *J. Am. Chem. Soc.*, 2017, **139**, 1690–1698." Copyright 2017 American Chemical Society.

Particle size dependence on CO oxidation on model planar titania supported gold catalysts measured by parallel infrared thermography

Small Au nanoparticles have been intensely studied for low-temperature CO oxidation.[94,95] For this reaction, high throughput IRT is an attractive method to screen multiple catalysts in parallel. Emmanuel *et al.*[96] utilized parallel IRT to measure CO oxidation over a series of amorphous titania supported Au catalysts to determine the effect of Au particle size on CO oxidation and to further elucidate the mechanism of CO oxidation using data from 100 different Au/TiO_2 catalysts. In order to well characterize this array-based system and obtain pertinent structure activity relationships, increased sensitivity is needed to detect heat generation during the reaction. Varying sized Au particles were deposited onto TiO_2 thin films (*ca.* 200 nm) by changing the total flux of gold to provide various thickness and different particle sizes.

The temperature response of the catalyst for a given power input was calculated through finite element thermal modeling. For the CO oxidation reaction ($\Delta H = -283$ kJ mol^{-1}) at a pressure of 1×10^{-3} mbar, the theoretical maximum power was determined to be 2.289×10^{-4} J s^{-1} mm^{-2}, which would result in a maximum temperature rise of 4 °C. Au particle distributions were measured using TEM and XPS, and film thickness of the TiO_2 support was measured using tapping mode AFM. To measure the TOF, the mass of gold and the number of gold atoms at the surface of the particles per area of catalyst was calculated from TEM images, assuming the particles are hemispherical. The chip containing 100 different Au particle sizes on TiO_2 was first heated to a base temperature of 170 °C. The total pressure of the gas mixture was 1.5 mbar with an O_2:CO ratio of 1:2. Fig. 6A shows the temperature distribution across the 100 catalysts for these reaction conditions. The catalysts were synthesized so that the particle size was consistent across the rows and varied along the columns, from 1.5 nm to 6 nm. Fig. 6B shows the variation in temperature change across each of the catalyst rows. The change in temperature for each row was *ca.* 0.2 °C, which was much smaller than the temperature change along the columns. From this figure, it is obvious to see an increase in the temperature change as the particle size decreases.

The TOF as a function of mean particle size was found to be highest for the smaller Au particles, and to monotonically

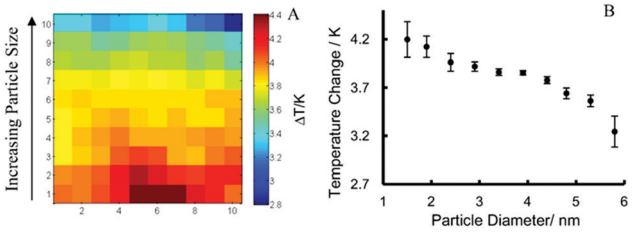

Fig. 6 (A) The temperature changes due to the CO oxidation reaction on an array of 100 Au/TiO_2 catalysts at 170 °C measured simultaneously with an infra-red camera. The total pressure of the gas mixture was 1.5 mbar and the O_2 : CO ratio was 1 : 2. (B) The average temperature rises over the ten catalysts with identical particle size. The errors represent the standard deviation in the 10 measurements. Adapted with permission from "The particle size dependence of CO oxidation on model planar titania supported gold catalysts measured by parallel thermographic imaging, *J. Catal.*, 2019, **369**, 175–180." Copyright 2019 Elsevier.

decrease as the particle size was increased. This same trend was also found for CO oxidation at 80 °C and at O_2 : CO ratio of 1 : 1. At 80 °C, 8.4×10^{-2} mbar, and an O_2 : CO ratio of 1 : 1, a TOF of 0.016 s^{-1} was observed for Au particles of 5.8 nm, and a TOF of 0.186 s^{-1} was observed for Au particles of 1.5 nm. For all reaction conditions studied, an increase in rate was found to be inversely proportional to the particle diameter.

Peripheral Au particles have been shown to strongly stabilize oxygen adsorbed on the reducible TiO_2 support, thus lowering the activation energy required for CO oxidation on nearby Au active sites.[97] To explore this relationship, the total particle circumference per surface area of TiO_2 was calculated from TEM images and plotted against the mean particle size, as shown in Fig. 7. Because circumference increases with mean particle size, the authors conclude that the number of edge sites at the Au/TiO_2 interface should also be proportional to

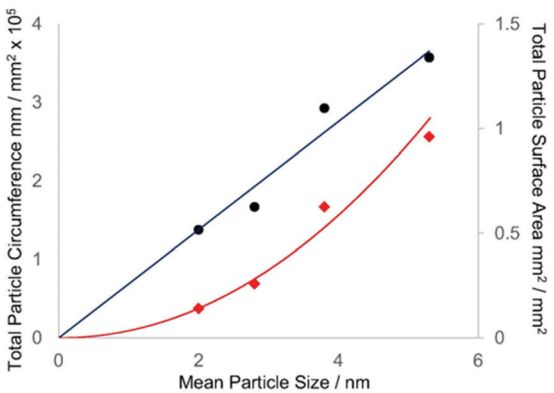

Fig. 7 The total circumference (mm) and surface area (mm^2) of particles (per mm^2 of titania support) calculated from the TEM images of titania supported Au nanoparticles for the four different deposition times, (a) 30 s, (b) 2 min, (c) 3.5 min and (d) 5 min corresponding to a mean particle size of (a) 2.0 nm, (b) 2.8 nm, (c) 4.5 nm, and (d) 5.3 nm. Particles were deposited at an Au deposition rate of 0.15 Å s^{-1} and a substrate deposition temperature of 200 °C. Adapted with permission from "The particle size dependence of CO oxidation on model planar titania supported gold catalysts measured by parallel thermographic imaging, *J. Catal.*, 2019, **369**, 175–180." Copyright 2019 Elsevier.

the circumference. This would result in a decrease in TOF with increasing density of Au/TiO_2 peripheral sites on the surface, suggesting that the high activity of these particles is unlikely due to the linear increase in Au edge sites. While it is generally accepted that the edge sites at the Au/TiO_2 interface play an important catalytic role in CO oxidation,[94,95,98,99] low coordinated Au sites and electronic modification of Au nanoparticles from the substrate may also play a role in improving low temperature catalytic activity. The authors conclude that the strong particle size dependence on TOF cannot be solely due to an increase in the number of edge sites at the Au/TiO_2 interface. The net increase in specific catalytic activity per surface area of Au was found to increase approximately as a function of d^{-4}. Therefore the authors determine that a significant metal–support interaction must largely account for this steep increase in activity that is observed with decreasing particle size.

Overall, these three examples show the effectiveness of different HT methodologies to investigate complex relationships present between synthesis variables, promoter materials, catalyst properties, and catalytic activity. While DoE has the ability to optimize a number of variables within a small experimental range, the information gained from studying trends cannot be utilized to derive consecutive experiments or used outside of their intended design space.

Machine learning – background

ML as a discipline arose from the desire to reproduce cognitive patterns inherent to rational thought in synthetic devices such as computers.[100,101] ML at its core is a combination of complex statistical algorithms that build a mathematical model from data in order to reason and predict outcomes without being explicitly programmed for the task at hand.[102] ML algorithms base their understanding on a user-provided database of prior knowledge, and from this data, the algorithm learns the consequences of all decisions made previously. It then uses these learned consequences to predict the outcome of choices that have never been made based on how similar those choices are to what the algorithm has experienced.

The ability of ML algorithms to learn relationships between choices and consequences is especially desirable for the scientific community. Specific to catalysis, there is a multitude of parameters that affect catalyst properties and ultimately performance, such as variations in the synthesis protocol, elemental composition, or operating conditions. The typical discovery process involves varying one or at best a few parameters within these categories to improve the desired properties of a material. DoE studies are typically employed to probe both the effects of these parameters and interaction effects between the parameters, but these studies often require hundreds of experiments to effectively screen even a small number of parameters. Sample efficient ML algorithms, on the other hand, can extract these parameter effects and interactions from smaller datasets, since they can leverage prior datasets. It is ideal, therefore, to develop a

machine learning framework capable of understanding parameter variation and learning the effects of parameters on various outcomes.

An effective ML framework is comprised of the following components: (1) a suitable ML model, (2) a dataset, and (3) a feature set, see Table 1. The first component of a ML framework, the selection of a ML model, is highly dependent on the dataset being used for learning. When a very large amount of data is accessible, algorithms such as DNNs are shown to have superior prediction accuracy compared to other algorithms. While a DNN produces accurate predictions, one major drawback is the difficulty to extract knowledge from these algorithms.[103] Consequently, DNN algorithms are frequently used in conjunction with other ML algorithms, such as affinity propagation[32] or decision trees,[104] to extract knowledge without sacrificing predictive capabilities. While DNNs are excellent algorithms, they require a sufficiently large dataset to achieve good performance. There are currently no means for determining the required dataset size, but some heuristics suggest maintaining high sample-to-feature ratios, such as greater than 10 samples per feature.[105] This restriction limits the usefulness of DNN, as most catalyst discovery datasets do not contain sufficient data for accurate predictions. There are some material properties that have entire databases cataloging composition–property correlations, for example, materials project catalogs the band-gap of over 50 000 materials.[106] Such open access databases allow for DNN models to be utilized, but the current scope of cataloged properties is unfortunately restrictively narrow for applications in heterogeneous catalysis.

Some ML algorithms are realistically employed on relatively small datasets, containing at times as few as 100 samples.[31] To select an optimal ML algorithm for small datasets, multiple algorithms are often evaluated to determine which has the highest performance. Of the available algorithms, ensemble algorithms,[107] support vector machines,[108] least absolute shrinkage and selection operator (LASSO),[109] and various regression algorithms[110] are used most commonly. Ensemble algorithms, such as random forests, involve training many models with random variation and using the average as the predicted value.[111] Support vector machines fit hyperplanes through multidimensional space, making them excellent algorithms for classification, although they have potential as a regression algorithm as well.[112] The LASSO algorithm is a regression analysis with inherent feature selection, which ultimately makes

Table 1 The components of an effective machine learning framework

(1) Selection of a suitable machine learning model		
Condition	Selection heuristic	Algorithms
Large dataset	Greater than 10 : 1 sample-to-feature ratio[105]	DNN
Small dataset	Less than 4000 samples[26]	Random forest Support vector machine (SVM) LASSO Regression algorithms
(2) Construction of a dataset		
Dataset option	Advantage	Disadvantage
Literature only	– Quickly create large database – Encompass many parameters	– Database is likely to be sparsely populated – May contain conflicting results – May contain inaccurate results – Often only includes positive results (successes)
Experimental only	– Dataset is consistent – Easier to evaluate results at same conditions	– Slow – Expensive
Combined literature and experimental	– Encompasses most data	– Sparse literature data may lead to inaccurate predictions away from experimental dataset – Larger experimental datasets may bias predictions, rendering sparse literature data irrelevant
(3) Selection of a feature set		
Feature type	Advantage	Disadvantage
Composition – Boolean	– Simple	– Does not capture full composition
Composition – loading	– Captures composition	– Typically only captures nominal loading
Bulk elemental – mean elemental value	– Simple – Captures elemental contribution	– Does not capture relative elemental contribution
Bulk elemental – weighted statistics	– Captures relative elemental contribution	– May be inaccurate if nominal does not match actual loading – Does not capture possible interaction effects between elements
Heuristics	– May help algorithm predictions – Can be used to evaluate heuristic accuracy	– May bias algorithm predictions – Possibility of heuristic being too general or too specific
Calculations – *a priori*	– Extremely accurate descriptor	– Often time consuming to calculate – May be inaccurate due to assumptions

the model easier to interpret by the user than other regression algorithms.[113] Regression algorithms mimic linear regression, but are augmented for better performance in multidimensional spaces.[114] None of the algorithms listed above are objectively better than the others in all cases; rather, each algorithm must be evaluated to determine which is best suited for modelling a particular dataset.[115,116]

The second component of a ML framework is the dataset itself. The construction of a dataset poses an interesting challenge for catalyst discovery. One option is to survey the available literature for a particular catalyst application and compile that literature into a database.[117] This collection provides a good starting point for ML, but it has multiple drawbacks. First, there is often a striking inconsistency in what is reported in the literature, even for matching catalyst compositions. Differing synthesis conditions lead to different catalysts, effecting properties such as crystal structure, particle size, and surface sites, among many others. These synthesis conditions are not always reported across studies, which leads to incomplete entries into the dataset. Second, the catalysts reported in the literature are often only those which are successful, leading to a strong bias in literature-generated datasets. For ML to effectively learn, the algorithm requires both positive and negative examples to be provided.[118] Ultimately, additional data would be required for a literature-generated dataset to make successful predictions and to distinguish between good and bad catalysts. Third, not all published data is good data.[119,120] Inclusion of data into the ML algorithms that are not accurate or reproducible will inevitably lead to inaccurate predictions, but there is no feasible way to evaluate every scientific claim when compiling a literature-based database. With all of these drawbacks, a careful assessment of the literature is necessary prior to any attempts to predict new catalyst compositions. Literature data may not be readily transferrable to the conditions or target variables that are desired.[118] Ultimately, additional data would be required for a literature-generated dataset to make successful predictions and distinguish between good and bad catalysts.

Alternatively, systematic experiments can be conducted to create a consistent, controlled dataset. A recent example of this approach was performed by Nguyen *et al.*, where 40 catalysts for oxidative coupling of methane were evaluated at 216 different conditions.[121] This approach can generate an ideal dataset for machine learning, since data trends are more easily identifiable when a majority of the experiment variables are held constant. Additionally, systematic experimentation allows for accurate validation of predictions, since the reactor and reaction conditions are already identical to the ML dataset. This approach, however, has the drawback of being more costly and time-consuming than simply accessing previous literature.

The third component of a ML framework is the feature set. The feature set is a compilation of characteristics describing the samples contained in the dataset. Compositional features are the most commonly included features for catalyst datasets. The composition can be indicated using Boolean values (0/1 indicate the absence/presence of the element) or mass fractions for each element on the periodic table (non-zero mass fraction indicates the element is present). Many groups use the mass fractions of elements to calculate weighted elemental properties, such as a weighted mean electronegativity.[122] Additionally, the range, minimum, maximum, and weighted mean absolute deviation of elemental properties have been included as features.[38] Some groups have included the properties of possible oxides, such as the enthalpy of formation or the element oxidation state within the oxide.[123,124] Other features, such as heuristics or fundamental theories, can also be included to increase model accuracy.[24] Large databases with derived or calculated values are also good candidates as features for machine learning.[125,126]

The focus of this perspective is on ML in experimental catalysis; however, it is worth noting that ML is also widely employed in computational catalysis as well.[70,127,128] Computational catalysis allows the design and testing of catalyst surfaces *in silico* and extraction of fundamental factors that heavily influence catalytic activity. Unfortunately, modeling these surfaces is very expensive, resulting in the study of only a few stable surface facets and possibly excluding other facets that contribute most to the reaction rate.[129] Machine learning techniques are being employed to reduce this bottleneck, accurately predicting new surface performance rather than constructing them *in silico.*[130] A recent, comprehensive review detailing the application of machine learning to computational catalysis can be found elsewhere.[131]

Application of machine learning in experimental heterogeneous catalysis

The application of ML to experimental catalysis began in the mid-1990s, when groups began exploring ML as a means to further increase the efficiency of their catalyst discovery process. Initially, the ANN algorithm was the primary algorithm explored.[100,132,133] Subsequently, groups explored GA, later augmenting the GA by coupling it with the ANN. Some groups also explored other machine learning algorithms, such as support vector machines and clustering algorithms. The following sections will explore and summarize some examples of this work.

Discovery of catalysts for the oxidative dehydrogenation of propane through genetic algorithms and artificial neural networks

One of the first applications of GA to catalysis was for the discovery of an optimal catalyst for the oxidative dehydrogenation of propane (ODP).[134] To optimize the GA parameters, a pseudo-dataset was constructed with defined equations that calculated a pseudo-conversion and pseudo-selectivity from the composition values of each catalyst. This pseudo-dataset was used to optimize a GA, identifying parameters such as the minimum population required to achieve successful results and the optimum number of elements per catalyst in the initial generation. These GA parameters were used to generate multiple generations during their experimental search for an optimal ODP catalyst. The initial population was comprised of 56 4-component catalysts. The 4 components of each catalyst were randomly

selected from a list of 8 elements, which were chosen based on prior knowledge of ODP, and their weight loadings were also randomly generated. This initial generation was tested experimentally using high-throughput techniques, and the propane conversion and selectivity towards propene were used to determine which catalysts would be used by the GA to seed the next generation through mutation and crossover (only catalysts with greater than 20% selectivity and 5% conversion were viable candidates). Continuing this procedure produced 4 total generations with 56 catalysts each. Notably, the mean propene yield increased with each successive generation, such that only 3 catalyst compositions failed the conversion and selectivity criteria in the final generation (compared to 19 compositions that failed in the first generation). Additionally, some elements from the initial 8 selected were almost entirely removed from the catalyst compositions by the final generation, indicating that the GA learned that these elements had a negative impact on the propene yield.

Despite the algorithm's success, there are some significant drawbacks. First, as stated by the authors, the 3rd generation of catalysts contained the highest yield, indicating that while the GA can learn and remove low propene yield catalysts, it isn't sufficient to predict catalysts with even higher yields. This is also evidenced by examining the composition of the final generation, where a majority of catalysts have similar compositions with only minor variations. The GA seems to converge on a particular composition and make minor changes from that optimal composition. In this regard, the initial application of GA to catalysis fails to be very different from standard high-throughput approaches, which screen a large design space for high performing catalysts and then explore the modification of other parameters in a much more confined parameter space.

The next approach was to apply artificial neural networks to the ODP dataset and determine composition-yield dependence.[135] The ANN used a single hidden layer, and the dataset was divided such that 75% of the data comprised the ANN training set and the remaining 25% of the data was available as a test set. Using these parameters, the model was able to achieve a mean absolute difference of 0.3% propene yield (relative 5.4% error to average propene yield). This value, however, is artificially low due to the similarity in the composition of the entire dataset. The authors addressed this point by predicting 6 new catalyst compositions with maximized propene yields using the ANN. They ensured the predicted compositions were different by varying the model hyperparameters, which causes the algorithm to converge at separate compositions. Testing these new catalysts and comparing the experimental values to the predicted values yields a new propene yield error of 1.1% (relative error 14%). A higher model error is expected for these new compositions, but the catalyst compositions predicted from this method do not appear novel or unique. All 6 best-predicted catalysts contain high amounts of Ga, ranging from 35–67%, and V, ranging from 17–41%. The best catalyst composition discovered through this methodology is $V_{17}Mg_{37}Mo_{11}Ga_{35}O_x$, which is similar to a high performing catalyst found through the previous GA screening ($V_{19}Mg_{39}Mo_9Ga_{33}O_x$). Consequently, this study shows that an ANN is capable of "memorizing" what is good but is not truly learning from the previous data. Additionally, datasets created by GA may not be suitable training sets for ANN, as the bias towards certain compositions appears to limit the ability of the ANN to predict outside of that range. The conclusion from this study is a list of heuristics for propene yield, such as "If 24% $<$ Ga $<$ 33% and..., then yield of propene $\geq$ 8%". These heuristics, while accurate in the determined parameter space, may not hold true at conditions other than those used in this study, and the inclusion of any additional possible elements would render the heuristics unhelpful.

In a final study one this dataset, a framework was designed to quickly tune a GA using ANN.[136] They use an ANN trained on catalyst compositions and measured propene yield to quickly predict the propene yield of each catalyst in a generation created by the GA. Using this approach, predicted propene yields may be used in place of experimental data to tune the GA hyperparameters. This saves time and reduces cost by mitigating catalyst synthesis and increasing the rate of GA convergence since optimal hyperparameters lead to catalyst discovery in fewer GA generations. One parameter that was examined in this study was the population size of each generation of catalysts. They determined from this study that population size is relatively unimportant to the convergence of the GA, whereby 11 generations, population sizes of 28, 56, and 280 catalysts each had achieved a similar maximum yield of propene. Additionally, the optimal catalyst composition achieved by each population size is similar in composition.

The use of ANN to tune GA is novel and promising, but this study does not provide enough information to truly validate the reported conclusions. The authors validate their ANN by extracting heuristics learned by the algorithm and then demonstrating experimental data that fit those heuristics, shown in Table 2. The 6 catalysts which are provided only vary in elemental composition by 1–2 mol% per element, while the heuristics themselves have elements that vary by as much as 12 mol%. Within a reasonably assumed experimental error, the catalyst compositions chosen by the authors are identical, and thus they are not sufficient to evaluate the ANN heuristics. The authors report that the model successful learns which elements make effective catalysts, as shown in Fig. 8, but this was already known about GA performance from prior studies. Noticeably absent is any report of the overall performance of the ANN on predicting the dataset, which would provide more understanding

Table 2 Experimental validation of rule 1 (examples 1–3) and rule 2 (examples 4–6) extracted from a trained ANN. Reproduced with permission from ref. 136

	Composition (mol%)				Propene yield (%)	
Example	Ga	Mg	Mo	V	Predicted	Experimental
1	32	32	7	29	8.1	8.2
2	27	36	6	31	8.1	8.4
3	32	33	5	30	8.3	8.0
4	38	31	8	23	8.3	7.9
5	38	31	9	22	8.4	8.3
6	38	32	9	21	8.4	8.2

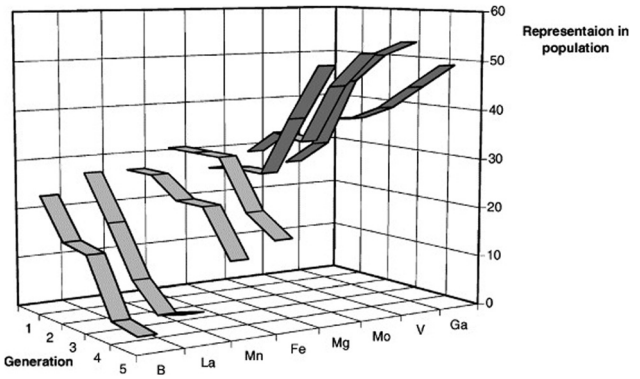

Fig. 8 The variation in the frequency that certain elements were contained within the predicted catalyst composition of the GA over the course of 5 generations. Copyright Elsevier 2004.

of the capabilities of the model to accurately predict the data. With this information lacking, it is entirely possible the observed convergence of each population size is a result of poor predictions from the ANN. Therefore, further investigation should be conducted in order to fully evaluate the effectiveness of this approach.

Genetic algorithms constrained by chemistry rules for extracting kinetic reaction parameters from the conversion of propane to aromatics over H-ZSM-5 catalysts

Caruthers *et al.* developed a coupled framework, combining GA with a reaction framework that includes 60 gas and surface species and 271 potential reaction steps.[43] The GA was used to search for and optimize a best-fit kinetic model, which was subsequently used to describe the weight fraction of the products at various reaction conditions. Each of the species and reaction steps was categorized into 13 groups to reduce the total number of features. The final feature set contained 9 rate constants (*e.g.* olefin desorption, k_{od}, or β-scission, k_b), 3 adsorption enthalpies (*e.g.* enthalpy change per carbon number for alkane adsorption, Δq_{ad}), and the entropy change for β-scission/oligomerization equilibrium. The GA was used to rapidly search this parameter space and locate optimal parameters that fit the experimental data. In total, the model identified 33 local minima with a similar sum of squares error (SSE), some of which contained drastically different values for certain kinetic parameters. For example, the rate of aromatization was reported to have an average value of 0.85 ± 0.90 mol g^{-1} h^{-1} across all the minima. This high error indicates that either this parameter is unimportant or that the model needs additional data to better understand this parameter.

Caruthers *et al.* began to expand the feature set, adding in additional terms from the full set of reaction steps and species. They found that adding one particular term, the alkylation of alkoxy species with light alkanes, caused the greatest improvement to the model by reducing the SSE, and the comparison of the original and refined model is shown in Fig. 9. Using this methodology of model refinement has the potential to uncover important factors influencing the reaction, and it has been demonstrated to significantly increase the accuracy of the model.

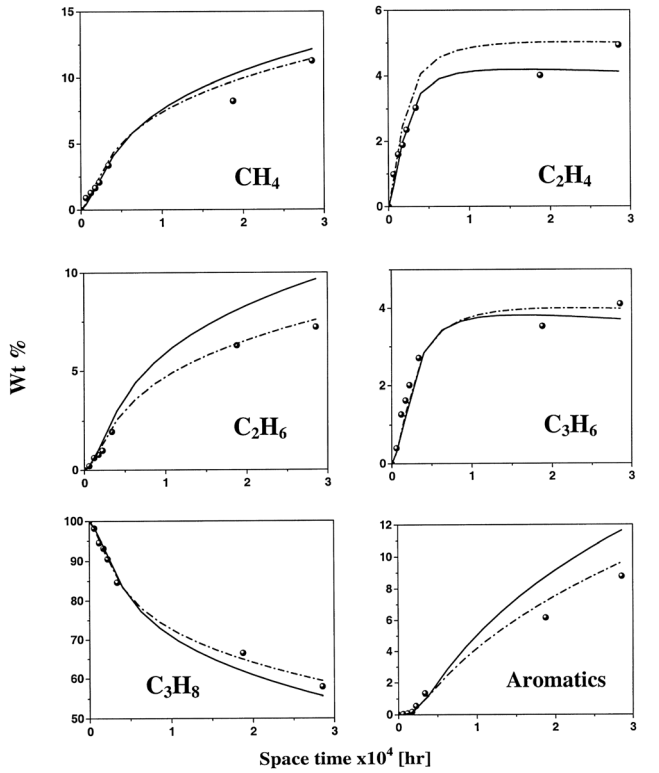

Fig. 9 Improvement in performance curves for propane aromatization on HZSM-5. Dots correspond to experimental data from Lukyanov *et al.*;[137] solid lines indicate the original model predictions and the dashed line indicate the refined model predictions. The *x*-axis is in terms of the space-time $\times 10^4$ (h) and the *y*-axis is the weight percentage of the various species. Copyright Elsevier 2003.

Despite these benefits, this application seems contradictory. The benefit of the GA is that it allows rapid searching of a diverse parameter space, but the original parameter space was simplified to the 13 categories to reduce the number of parameters. This, followed by a stochastic search for the next best feature, raises questions of why a GA was not implemented on the entire parameter space in the first place. It seems that this initial simplification artificially constrains the model, and likely limits the effectiveness of the GA. Needless to say, the authors do not provide an explanation for this choice in methodology.

Finally, the authors propose a knowledge mapping component to their framework, where these kinetic parameters are mapped to fundamental catalyst descriptors, such as proton affinity or transition state geometries. They do not demonstrate how, for this particular example, this knowledge extraction process works; rather, they create a hypothetical example where they compare the predictions of a typical ANN implementation with an ANN constrained by extracted knowledge. The hybrid model, containing the expert knowledge, had a much better fit than the typical model when it was extrapolated from their hypothetical data points. This shows the potential for knowledge extraction to inform predictive models; however, the study still leaves the demonstration of this feat to be shown.

Artificial neural network boosted genetic algorithms for optimization of Ti-silicate synthesis parameters for olefin epoxidation

Corma *et al.* used an ANN combined with a GA and HTE to optimize multiple catalyst systems, including catalysts for the oxidative dehydrogenation of ethane,[138] water–gas shift catalysts,[139] and the synthesis variables of a Ti-silicate olefin epoxidation catalyst.[140] In the latter study, four synthesis variables were selected: gel pH, hexadecyltrimethylammonium hydroxide content, tetramethylammonium hydroxide content, and titanium content. Their group reported previously that the primary factor impacting the success of a GA is the diversity of the initial generation.[141] Therefore, they used multiple GA to create several random catalyst generations and manually selected a diverse initial population. The GA was used to create new generations from the initial catalyst population, and an ANN was used to predict and pre-screen each new catalyst compositions. The authors iterated through 3 generations of catalysts with varied synthesis parameters. Over the 3 generations, the GA-ANN approach was able to optimize the synthesis parameters to increase the epoxide yield from ~92% to ~95% at a reaction temperature of 333 K. Select samples were chosen for a post-analysis *via* X-ray diffraction, which revealed a Ti-silicate structure that correlated strongly to catalyst activity. This study is one of the earliest studies to bridge the gap between catalyst synthesis and crystal structure with machine learning techniques.

In a later study, Corma *et al.* used data from the Ti-silicate study described above to explore a number of other machine learning techniques, comparing the performance of machine learning models using logistic regression equations to both neural networks and decision trees.[142] The features used to train these models were also varied, using combinations of catalyst synthesis and characterization features. Specifically, they applied dimensionality reduction techniques, such as principal component analysis and Kohonen networks, to X-ray diffraction (XRD) data collected on the catalysts. Accuracy of the model was obtained by comparing catalyst classifications assigned by the models, with 5 categories ranging from ''very bad'' to ''very good''. The validation was conducted with a pseudo-5-fold cross-validation, where 80% of the data was used to train and 20% to test, but the data for each validation was independently selected for the 80–20% split at random, unlike a typical cross-validation strategy. Inclusion of the dimensionally reduced XRD data increased the prediction accuracy of the ANN to 94%, and decision trees were able to achieve 100% prediction accuracy. It is important to note that, since the dataset being leveraged for this study was generated from a GA, a large portion of the dataset has similar catalyst parameters with minor variations, which will artificially inflate the ability of the machine learning models to make accurate predictions. A better test would have been to ensure predictions were made on vastly different parameters so that the actual predictive ability of the model could be probed. Nevertheless, this is the first study to include characterization, such as XRD, in a predictive model. This framework paves the way for more studies to incorporate characterization techniques and provide fundamental insight into the catalyst surface to the machine learning model.

In another study, the application of support vector machine (SVM) as a classification technique to two previously collected datasets, their olefin epoxidation dataset and their light olefin isomerization dataset, was explored.[34] The olefin epoxidation dataset was chosen because it is well dispersed, with yields ranging from 0–95% and about half the data being above 80% yield. They chose this midpoint as a classification threshold, where the aim was to distinguish good and bad catalysts. The isomerization dataset, on the other hand, ranges from 0–50% yield, but only 15% of the data has a yield higher than 5% and a majority of the dataset has a 0% yield. The threshold for this classification problem was set at 5% yield to classify active and inactive catalysts. They compared the performance of 8 SVM algorithms to 6 different classification tree algorithms for both datasets. In both cases, the RBF3 SVM algorithm outperformed all other SVM and classification tree algorithms, achieving near-perfect classification accuracy for both datasets. Both datasets were generated using a GA approach, which, as mentioned with previous studies, leads to concern about the homogeneity of the datasets and how well these classifiers actually perform in realistic situations.[143] Despite this concern, the authors demonstrate the accuracy of SVM to their dataset and ascribe its performance to the inherent mitigation of model overfitting, which is especially prevalent on small datasets for algorithms such as ANN.

Random forest algorithms for discovery of novel ammonia decomposition catalysts

Recently, our group developed a random forest-based ML framework in combination with high-throughput screening (ML-HTE) for accelerated catalyst discovery.[144] This methodology was successfully employed to predict the ammonia conversions of previously unknown catalyst compositions. A design space was centered around modifying a 12 wt% K promoted 4 wt% Ru catalyst supported on γ-Al_2O_3 (4,12 RuK/Al_2O_3) previously reported in the literature.[145] This catalyst was selected for the exploration of elements that may act to enhance low-temperature ammonia decomposition activity at lower Ru loadings than the previously reported 4,12 RuK/Al_2O_3 catalyst. Fig. 10 shows a compilation of most of the active metals studied for ammonia decomposition from 2001 to 2018. The focus for ammonia decomposition catalysts has predominantly been on Ru, and thus very little work has been done involving other transition, late transition or noble metal catalysts, let alone binary or even ternary combinations of these materials. The lack of comprehensive data under reproducible conditions made the selection of a starting point for this design difficult. If this were to be done with a traditional DoE, determination of a center point would involve very little scientific evidence and much guesswork, resulting in many failed experiments in addition to a much smaller design space than can be explored by a ML algorithm. The modifications to the centerpoint catalyst included replacement of a fraction of Ru with 1 of 33

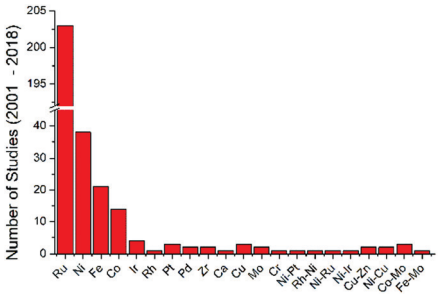

Fig. 10 Compilation of active metals studied for ammonia decomposition literature from 2001 to 2018. References may be provided upon request.

other elements and varying the ratio of Ru to substituted element present in the catalyst. Due to the flexibility of ML, we were able to define 33 different elements, each with three different weight loading or "levels". This kind of design would be difficult to realize with a traditional DoE due to a large number of categorical variables. Additionally, no meaningful relationships could be ascertained between activity and substituted metals using traditional DoE, because the relationships involve multiple properties of the elements and reaction conditions.

We utilized ML to deduce what combinations of materials and weight loadings would be most effective for low-temperature ammonia decomposition without having to synthesize and test hundreds of catalysts. The ML algorithm utilized information on elemental properties, synthesis conditions, and operating conditions to make predictions of the activity of substituted Ru catalysts. The training data for the ML was generated *via* a 16-channel HT reactor.[64,65,146] The initial training dataset included a base composition of 3 wt% Ru and 12 wt% K co-impregnated onto γ-Al_2O_3 in addition to either 1 wt% Ca, Mn, or In. The elements Ca, Mn, and In were chosen to maximize the difference in features in the initial dataset since those elements reside in three different categories on the periodic table (alkaline earth metal, transition metal, and post-transition metal). Unlike prior algorithms, which used predominantly catalyst composition as an input, and our framework included weighted elemental features, such as electronegativity or ionization energy, for each catalyst composition. The use of these additional features allowed the ML to accurately rank the catalyst formulations based on their expected performance with only 3 catalysts in the initial training set. The model made these predictions based on features which describe the catalyst's electronic, elemental, and geometric properties. After the predictions were made, the data set was synthesized and tested to validate the qualitative and quantitative accuracy of the model.

This ML-HTE framework led to the discovery of several novel high-performing catalyst formulations, such as a 3% Ru, 1% Y, 12% K catalyst on γ-Al_2O_3 (3,1,12 RuYK). Fig. 11 shows the catalytic activity of the newly discovered Y containing catalysts compared to the thermodynamic limit between 250 °C and 400 °C. The substitution of Ru with as much as 3% Y (1,3,12 RuYK) further resulted in a highly active catalyst at low reaction temperatures ($\leq$400 °C) for ammonia decomposition.

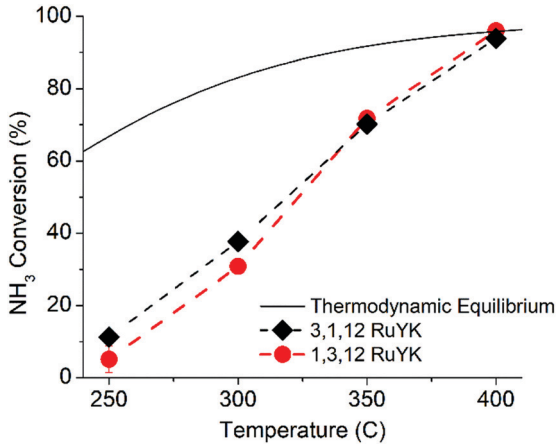

Fig. 11 Catalytic activity of 3% Ru, 1% Y, 12% K on γ-Al_2O_3 (black diamonds) and 1% Ru, 3% Y, 12% K on γ-Al_2O_3 (red circles) compared to the thermodynamic equilibrium conversion at atmospheric pressure. Reaction conditions: 100% NH_3, P = 1.01 bar, 5200 mL h^{-1} g_{cat}^{-1}.

The Y containing catalysts were compared to the best catalysts reported in the literature for ammonia decomposition at identical reaction conditions.[147] Using 7 wt% Ru supported on carbon nanotubes, they reported activity of roughly 80% conversion at 400 °C, compared to 94% and 95% conversion obtained with our 3,1,12 RuYK and 1,3,12 RuYK catalysts respectively. Additionally, the novel catalyst formulations discovered through ML-HTE achieved nearly double the ammonia conversion at temperatures as low as 250 °C and 300 °C using only one-seventh of the Ru content. The excellent performance of the ML-HTE framework led to the rapid discovery of new catalysts for low-temperature ammonia decomposition. With the addition of subsequent experiments, the ML design space may be further expanded to include variables such as catalyst support, synthesis parameters, and promoter type and loading. This opens the door for hyper-accelerated catalyst discovery that is only possible with the utilization of ML to predict catalyst formulations using a data set size reasonably achieved through high-throughput experiments.

It is interesting to note that the model used here is agnostic of the reaction chemistry and made accurate predictions without any information on reaction kinetics or adsorbate binding energies. While some theoretical ML studies utilize binding energies, Fermi level, or d-band center location in their feature selection process,[148,149] these energies are for well defined monometallic or bimetallic catalyst surfaces.[150] The complexity of the catalysts studied here and the ambiguity of the role of each catalyst component makes calculations of binding energies for these catalysts complicated. However, an estimation of the adsorbate metal interaction energies may only be necessary to enhance catalyst predictions. Recently it has been shown that integrating approximations for band gap, lattice thermal conductivity, and elastic properties into a ML model dramatically improved the predictive capability[31] for small data sets. Open source calculations and libraries of adsorbate binding energies using ML algorithms are beginning to arise,[33,151] but

the generalizability and influence of variables such as metal support interactions and particle size have yet to be addressed. The utilization of ML not only for catalyst predictions but also for predicting metal adsorbate interactions for more complex surfaces and catalysts compositions in a cost-effective and efficient manner, would dramatically enhance material discovery and pave the way for catalyst discovery containing three and four components in lieu of the traditional active metal and promoter combination.

New advances in machine learning algorithms

The catalyst discovery process involves many decisions about process design, operation, and catalyst properties, where experimentation plays a pivotal role in evaluating these decisions. Traditionally, these decisions were aided by methodologies, such as DoE,[152,153] but the trend in research towards increasingly complex catalysts has begun to render these traditional techniques impractical or even infeasible due to time and cost restrictions.[154] The search for an optimal catalyst involves interactions between a multitude of variables, leading to a complex search problem over a massive configuration space with multiple objectives involved (we are interested to find stable, active, and low cost catalysts).[154] Computational evaluations are usually less costly to perform than physical experiments, allowing a lower cost iterative search process. In the absence of analytical knowledge about the material synthesis process (such as those that can be obtained through DFT, finite element analysis, or computational fluid dynamics), we can approach the problem of material synthesis as a black-box problem, where ML is best suitable for solving such problems. Here, we will shed light on the use of novel ML and data-driven approaches in catalyst design. We will discuss active learning for an iterative design process and transfer learning to accelerate the discovery process. We will also discuss causal inference for enhancing catalyst design to not only suggest potential catalyst formulations but to also provide chemical explanations for such choices. We will finally discuss the infrastructure for enabling data-driven discovery at scale. Note that we will keep the discussion here at a high level and we do not intend to provide in-depth analysis. Rather, we want to provide insights into opportunities for future research based on existing work in the literature.

Active learning (sequential design)

On an abstract level, catalyst design problems are primarily concerned with the evaluation of a complex function, which maps features describing the catalyst composition to some chemical process. In this scenario, the complex relationship between the catalyst features and the catalyst performance is unknown, which renders optimization a major challenge and requires sampling of the performance for multiple iterations of catalyst features. The main obstruction in such a design and many other contexts is that the typically large dimensionality of the parameter space requires, in general, an enormous number of samples to derive reliable optimality conclusions, *i.e.* the curse of dimensionality.

One possible solution to minimize the required number of samples is Bayesian optimization, which is a ML framework used to optimize expensive black-box functions. This methodology has been used previously for iterative (sequential) experimental designs.[155] The black-box function is typically modeled *via* a Gaussian process (GP), building a mathematical model from available experimental data, and then using this model to recommend the next set of experimental parameters, giving rise to an iterative approach. At each iteration, the uncertainty captured by the probabilistic model is used to generate a utility function, where the optimal point of this function is the set of parameters most likely to increase the accuracy of the predictions. Unlike the actual objectives, the utility function is a function of the model and, therefore, it is cheap to evaluate and maximize. This approach contrasts with model-free approaches, such as genetic algorithms or evolutionary strategies, that can be effective for approximating the Pareto set but require many function evaluations with prohibitive cost in materials design applications. The GP is updated with new data as experiments are conducted. In this context, Bayesian optimization was shown to have the best achievable order of convergence rate in terms of the number of samples (sub-linear growth in cumulative regret) for global optimization.[156,157] It can be applied to high-dimensional optimization of general types and more importantly, it offers transfer learning from past experiments in an efficient optimization framework.[158]

Transfer learning

The process of experimentation involves conducting an experiment, measuring the quality of output, then repeating the process with insights gained. This process is inherently iterative, dynamic, expensive, and limited by resources of time, cost and even ideas. Knowledge is built over time through several sets of experiments that vary in setting – thus ''similar'' experimental data is often available. For example, in catalyst discovery, there is typically a wealth of experimental and computational data available for a particular catalyst system. These data should contain information that is transferable to the current discovery effort. In particular, existing data can be used in a setting that enables transfer learning with Bayesian optimization.[159] Also, we can transfer knowledge from low-fidelity experiments and numerical simulations to enhance the multi-fidelity Bayesian optimization process (see Fig. 12). In particular, multi-fidelity Bayesian optimization enables transfer learning from less expensive low-fidelity simulations/experiments and enables a more accurate prediction of material properties and, therefore, more efficient discovery process that learns jointly from both low-fidelity and high-fidelity data.[159–163] We see an enormous potential in this approach that would result in a more accurate exploration of the performance landscape with an improved chance of detecting ''unexpected'' catalyst compositions.

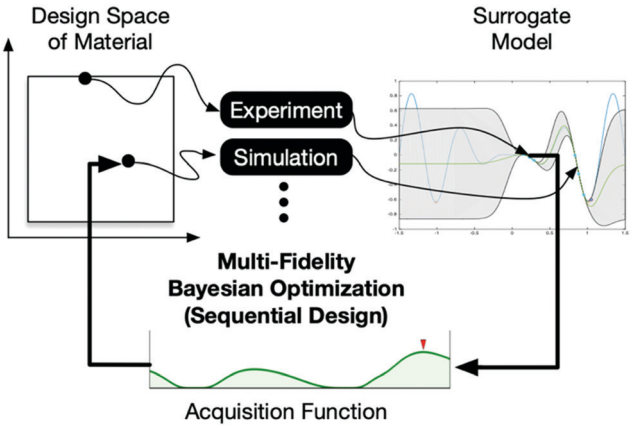

Fig. 12 Sequential design with Bayesian optimization and transfer learning.

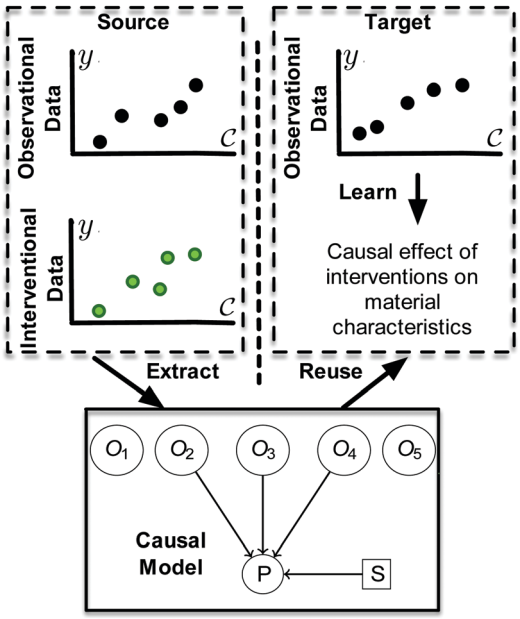

Fig. 13 Extracting knowledge from the source environment and transferring to the target environment for causal discovery.

Explainability and causal inference

Integrating AI techniques with pipelines for catalyst discovery involves communicating the extracted knowledge with both experimentalists and theoreticians. Here we explain challenges and a possible approach to overcome them using causal modeling tools, in particular, causal inference[164] and their associated logic. Causal inference facilitates identifying the causes of an observed outcome *via* interventions and counterfactual analysis. We believe that these tools enable efficient communication of the knowledge that we extract from the catalyst discovery process.

The first challenge is adaptability, or robustness, of the machine learning algorithm. Many current machine learning implementations lack the ability to accurately extrapolate outside of the design space that they have been specifically trained for. Transfer learning and domain adaptation are both novel techniques that address the issue of adaptability by incorporating additional datasets into the machine learning process.[165–168] Causal information[165] and probabilistic information collected from current experiments (*i.e.*, the catalysts we already collected data from) can be used to extract knowledge, predict, and infer properties about new target experiments,[169] therefore, saving time and cost if the inferred information indicates that the catalyst is not going to possess certain properties of interests. Common intuition supported by previous research suggests that from the limited probabilistic information about the target catalyst *via* the synthesis results, we may be able to infer that certain probabilistic and causal facts are shared between the two processes and certain ones are not. Conclusions about one population can be supported by information about another but depends on exactly what causal and probabilistic facts they have in common (see Fig. 13).

A second challenge is explainability, which deals with the inner working of the machine learning algorithm and why it predicts certain catalysts to be good while others to be bad.[170] Most current algorithms rely on the researchers' intuition to evaluate what constitutes a good explanation, impeding diagnosis and repair.[171,172] However, a model-based approach using structural causal models (also known as Structural Equation Models)[173] to internally evaluate cause–effect relationships can cast new light on the question of what constitutes an adequate explanation, and it opens new possibilities for the automatic generation of explanations by machines.[174] Causal models can then be used to communicate the extracted knowledge. Causal relations are typically specified using structural causal models such as $A \rightarrow B \rightarrow C$ or $A \rightarrow B \leftarrow C$, is $Y = f(X,\varepsilon)$, wherein the former B mediates the change from A to C and in the latter B blocks the correlation between A and C, and ε is the error term. Such causal structures can be used to better guide the optimization process using targeted sampling or improving the reliability of models when the underlying mechanisms change across environments.[175]

A third challenge regards the lack of machine understanding for cause–effect relationships. Machine learning algorithms have been primarily designed to answer questions of a statistical nature, such as "What is the probability that A occurs?", but equally important is the ability to answer questions of a more philosophical nature – "What if?"-type questions.[176] The ability to ask and answer these "what-ifs" separates standard machine learning from true AI. Examples include interventional questions: "What if we set the number of specific components to a certain level in an experiment?" or "What if we put more of component X instead of component Y and observe how the characteristics of the derived material will change?" Counterfactual questions involving retrospection cannot be directly answered from data collected by interventions or controlled experiments.[177] To address this challenge, the structural causal model can be used to answer counterfactual questions using both experimental studies and the structure of the causal diagram in combination of Judea Pearl's Do-Calculus.[176]

We prescribe causal modeling and counterfactual reasoning to overcome all three challenges in the application of machine

learning to catalyst synthesis and optimization, in particular, causal diagrams and their associated logic. These tools could complement the ML models by providing explanations regarding the decisions produced by the models, learning a better representation that transfer better across environments,[178] or even enhance the models by disentangling the causal factors that explain the variation in the data in order to build robust models.[179] The causal models can also be integrated into the iterative Bayesian optimization that derive experiments to increase the chance of discovering new materials and provide explanations. Through addressing these challenges, AI algorithms for catalyst discovery will not only be able to predict novel materials, as has been shown previously, but will also have the capacity to ask scientific questions, evaluate which questions are most important, and design experiments to generate knowledge and improve understanding.[25,180–187]

High capacity machine learning

Experimental data from multiple groups, databases of HT data, and extraction of data from the literature can all generate significant amounts of data and as a result, training deep neural network (DNN) (or in general any ML model) can be resource-intensive. DNN models are trained using a backpropagation algorithm, which computes the error signal of each parameter in the model and uses it to adjust the parameters according to gradient descent algorithms. The training process is inherently iterative, where training batches are processed sequentially. DNN models typically have thousands or millions of parameters. Therefore, training deep learning models on big data is challenging due to the computational demands of our data-driven strategy. Even with a powerful GPU, some models can take days or weeks to train. Fortunately, given cloud services, we can have access to multiple machines and multiple GPUs. To scale the training process, we can adopt distributed ML training by leveraging powerful heterogeneous hardware environments to achieve significant acceleration.[188] In doing so, first, the generated experimental data is transferred to the cloud. In the distributed cloud-based architecture (Fig. 14), we can partition the data over multiple cloud nodes that may be hosted on different cloud platforms. Then, the probability density function of all variables including density, velocity, energy, and scalars will be batched for deep learning analysis.

To describe the methodology, assume there are n nodes, then each node will receive a copy of the complete model and train it on $1/n$ of the data. At a high level, each node trains on its own fragment of data and generates a set of parameter updates. Then, a global parameter state is created from the ensemble of parameter sets created by the nodes. The new gradients and updated model are communicated across these nodes using Apache Spark cluster primitives (see Fig. 14). In order to deal with big data generated here, we need to resort to Hadoop Distributed File System (HDFS) on multi-cloud. This means of storage allows direct access to the data and seamless interoperability between various services such as Spark and Google services. This will save significant cost over time and enable high capacity machine learning at scale with big data from multiple groups, databases of experimental and theoretical HT data, and extraction of data from the literature.

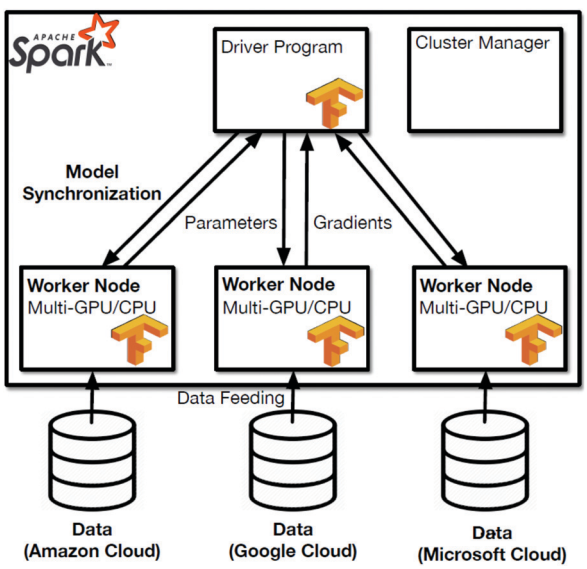

Fig. 14 Computational infrastructure for high capacity machine learning.

Conclusions

There are many advances in high-throughput methodologies that allow the researcher to rapidly synthesize and screen catalysts. While combining such HT methodologies with DoE allows one to interpolate and search for local maxima within a given parameter space, it does little to accelerate the rate of previously unknown materials discovery for experimental catalysis. In contrast, catalyst discovery has been demonstrated for a few select cases using various machine learning based algorithms, including GAs, ANNs, and random forest algorithms. Limitations still exist when extending catalyst discovery to the synthesis of real materials. We demonstrated that the combination of random forest algorithms with high-throughput screening can result in successful material discovery for ammonia decomposition catalysts. The addition of generalized parameters, such as adsorbate binding energies, band gap, or reaction kinetics could further improve the predictability of machine learning models. Additionally, there exist opportunities in the future for transfer learning from computational data to lead to more accurately predict performance of existing and novel catalyst formulation. The most exciting opportunities, however, lie in the extraction of new knowledge from such large datasets in the form of causal models, exploring multi-dimensional connections between catalyst features in a explainable and reliable fashion.

Conflicts of interest

There are no conflicts to declare.

Acknowledgements

This work was supported by APRA-E DE-AR0000931. T. W. and K. M. were supported by NSF Integrative Graduate Education and Research Traineeship grant no. 1250052.

Notes and references

1 R. Potyrailo and E. Amis, Elements of High-Throughput Analysis, in *High-Throughput Analysis: A Tool for Combinatorial materials Science*, Kluwer Academic Publishers, 2003, pp. 1–14.
2 A. Mittasch and W. Frankenburg, Early studies of multicomponent catalysts, *Adv. Catal.*, 1950, **2**, 81–104.
3 J. J. Hanak, The ''multiple-sample concept'' in materials research: synthesis, compositional analysis and testing of entire multicomponent systems, *J. Mater. Sci.*, 1970, **5**(11), 964–971.
4 J. G. Creer, P. Jackson, G. Pandy, G. G. Percival and D. Seddon, The design and construction of a multichannel microreactor for catalyst evaluation, *Appl. Catal.*, 1986, **22**(1), 85–95.
5 W. F. Maier, Early years of high-throughput experimentation and combinatorial approaches in catalysis and materials science, *ACS Comb. Sci.*, 2019, **21**(6), 437–444.
6 P. Chen, Electrospray ionization tandem mass spectrometry in high-throughput screening of homogeneous catalysts, *Angew. Chem., Int. Ed.*, 2003, **42**(25), 2832–2847.
7 M. T. Reetz, New methods for the high-throughput screening of enantioselective catalysts and biocatalysts, *Angew. Chem., Int. Ed.*, 2002, **41**(8), 1335–1338.
8 J. G. de Vries and A. H. M. de Vries, The Power of High-Throughput Experimentation in Homogeneous Catalysis Research for Fine Chemicals, *Eur. J. Org. Chem.*, 2003, 799–811.
9 M. Renom-Carrasco and L. Lefort, Ligand libraries for high throughput screening of homogeneous catalysts, *Chem. Soc. Rev.*, 2018, **47**(13), 5038–5060.
10 M. Shevlin, Practical High-Throughput Experimentation for Chemists, *ACS Med. Chem. Lett.*, 2017, **8**(6), 601–607.
11 M. Shevlin, M. R. Friedfeld, H. Sheng, N. A. Pierson, J. M. Hoyt, L. C. Campeau and P. J. Chirik, Nickel-Catalyzed Asymmetric Alkene Hydrogenation of α,β-Unsaturated Esters: High-Throughput Experimentation-Enabled Reaction Discovery, Optimization, and Mechanistic Elucidation, *J. Am. Chem. Soc.*, 2016, **138**(10), 3562–3569.
12 I. Petousis, D. Mrdjenovich, E. Ballouz, M. Liu, D. Winston, W. Chen, T. Graf, T. D. Schladt, K. A. Persson and F. B. Prinz, High-throughput screening of inorganic compounds for the discovery of novel dielectric and optical materials, *Sci. Data*, 2017, **4**(1), 160134.
13 M. Green, I. Takeuchi and J. Hattrick-Simpers, Applications of high throughput (combinatorial) methodologies to electronic, magnetic, optical and energy-related materials, *J. Appl. Phys.*, 2013, **113**(23), 1–53.
14 P. Cai, X. Zhang, M. Wang, Y. L. Wu and X. Chen, Combinatorial Nano-Bio Interfaces, *ACS Nano*, 2018, **12**(6), 5078–5084.
15 J. J. Haven, E. Baeten, J. Claes, J. Vandenbergh and T. Junkers, High-throughput polymer screening in microreactors: boosting the Passerini three component reaction, *Polym. Chem.*, 2017, **8**(19), 2972–2978.
16 Z.-H. Shen, J.-J. Wang, Y. Lin, C.-W. Nan, L.-Q. Chen and Y. Shen, High-Throughput Phase-Field Design of High-Energy-Density Polymer Nanocomposites, *Adv. Mater.*, 2018, **30**(2), 1–6.
17 Y. Zhou, Q. Li, B. Dang, Y. Yang, T. Shao, H. Li, H. Jun, R. Zeng, J. He and Q. Wang, Polymer Dielectrics: A Scalable, High-Throughput, and Environmentally Benign Approach to Polymer Dielectrics Exhibiting Significantly Improved Capacitive Performance at High Temperatures, *Adv. Mater.*, 2018, **30**(49), 1–7.
18 D. B. Miracle and O. N. Senkov, A critical review of high entropy alloys and related concepts, *Acta Materialia*, Elsevier Ltd, 2017, vol. 122, pp. 448–511.
19 O. N. Senkov, J. D. Miller, D. B. Miracle and C. Woodward, Accelerated exploration of multi-principal element alloys with solid solution phases, *Nat. Commun.*, 2015, **6**(6529), 1–10.
20 M. McBride, N. Persson, E. Reichmanis and M. Grover, Solving Materials' Small Data Problem with Dynamic Experimental Databases, *Processes*, 2018, **6**(7), 79.
21 K. Takahashi, I. Miyazato, S. Nishimura and J. Ohyama, Unveiling Hidden Catalysts for the Oxidative Coupling of Methane based on Combining Machine Learning with Literature Data, *ChemCatChem*, 2018, **10**(15), 3223–3228.
22 M. J. Cheng, E. L. Clark, H. H. Pham, A. T. Bell and M. Head-Gordon, Quantum Mechanical Screening of Single-Atom Bimetallic Alloys for the Selective Reduction of CO2 to C1 Hydrocarbons, *ACS Catal.*, 2016, **6**(11), 7769–7777.
23 A. G. Kusne, T. Gao, A. Mehta, L. Ke, M. C. Nguyen, K. M. Ho, V. Antropov, C. Z. Wang, M. J. Kramer, C. Long and I. Takeuchi, On-the-fly machine-learning for high-throughput experiments: Search for rare-earth-free permanent magnets, *Sci. Rep.*, 2014, **4**(1), 6367.
24 F. Ren, L. Ward, T. Williams, K. J. Laws, C. Wolverton, J. Hattrick-Simpers and A. Mehta, Accelerated discovery of metallic glasses through iteration of machine learning and high-throughput experiments, *Sci. Adv.*, 2018, **4**(4), eaaq1566.
25 K. Tran and Z. W. Ulissi, Active learning across intermetallics to guide discovery of electrocatalysts for CO_2 reduction and H_2 evolution, *Nat. Catal.*, 2018, **1**(9), 696–703.
26 D. Jha, L. Ward, A. Paul, W.-k. Liao, A. Choudhary, C. Wolverton and A. Agrawal, ElemNet: Deep Learning the Chemistry of Materials From Only Elemental Composition, *Sci. Rep.*, 2018, **8**(1), 1–13.
27 S. Brin and L. Page, The Anatomy of a Large-Scale Hypertextual Web Search Engine, *Comput. Networks ISDN Syst.*, 1998, **30**(1–7), 107–117.
28 V. Mnih, K. Kavukcuoglu, D. Silver, A. A. Rusu, J. Veness, M. G. Bellemare, A. Graves, M. Riedmiller, A. K. Fidjeland, G. Ostrovski, S. Petersen, C. Beattie, A. Sadik, I. Antonoglou, H. King, D. Kumaran, D. Wierstra, S. Legg and D. Hassabis,

Human-level control through deep reinforcement learning, *Nature*, 2015, **518**(7540), 529–533.

29 J. De Fauw, J. R. Ledsam, B. Romera-Paredes, S. Nikolov, N. Tomasev, S. Blackwell, H. Askham, X. Glorot, B. O'Donoghue, D. Visentin, G. van den Driessche, B. Lakshminarayanan, C. Meyer, F. Mackinder, S. Bouton, K. Ayoub, R. Chopra, D. King, A. Karthikesalingam, C. O. Hughes, R. Raine, J. Hughes, D. A. Sim, C. Egan, A. Tufail, H. Montgomery, D. Hassabis, G. Rees, T. Back, P. T. Khaw, M. Suleyman, J. Cornebise, P. A. Keane and O. Ronneberger, Clinically applicable deep learning for diagnosis and referral in retinal disease, *Nat. Med.*, 2018, **24**(9), 1342–1350.

30 R. Schmack, A. Friedrich, E. V. Kondratenko, J. Polte, A. Werwatz and R. Kraehnert, A meta-analysis of catalytic literature data reveals property-performance correlations for the OCM reaction, *Nat. Commun.*, 2019, **10**(1), 1–10.

31 Y. Zhang and C. Ling, A strategy to apply machine learning to small datasets in materials science, *npj Comput. Mater.*, 2018, **4**(1), 28–33.

32 Z. Li, S. Wang, W. S. S. Chin, L. E. E. Achenie and H. Xin, High-throughput screening of bimetallic catalysts enabled by machine learning, *J. Mater. Chem. A*, 2017, **5**(46), 24131–24138.

33 B. Meyer, B. Sawatlon, S. Heinen, O. A. Von Lilienfeld and C. Corminboeuf, Machine learning meets volcano plots: Computational discovery of cross-coupling catalysts, *Chem. Sci.*, 2018, **9**(35), 7069–7077.

34 L. A. Baumes, J. M. Serra, P. Serna and A. Corma, Support vector machines for predictive modeling in heterogeneous catalysis: A comprehensive introduction and overfitting investigation based on two real applications, *J. Comb. Chem.*, 2006, **8**(4), 583–596.

35 K. Huang, F.-Q. Chen and D.-W. Lü, Artificial neural network-aided design of a multi-component catalyst for methane oxidative coupling, *Appl. Catal., A*, 2001, **219**(1–2), 61–68.

36 Z. W. Ulissi, M. T. Tang, J. Xiao, X. Liu, D. A. Torelli, M. Karamad, K. Cummins, C. Hahn, N. S. Lewis, T. F. Jaramillo, K. Chan and J. K. Nørskov, Machine-learning methods enable exhaustive searches for active Bimetallic facets and reveal active site motifs for CO_2 reduction, *ACS Catal.*, 2017, **7**(10), 6600–6608.

37 A. F. Zahrt, J. J. Henle, B. T. Rose, Y. Wang, W. T. Darrow and S. E. Denmark, Prediction of higher-selectivity catalysts by computer-driven workflow and machine learning, *Science*, 2019, **363**(6424), 1–11.

38 L. Ward, A. Agrawal, A. Choudhary and C. Wolverton, A general-purpose machine learning framework for predicting properties of inorganic materials, *npj Comput. Mater.*, 2016, **2**, 16028.

39 R. Wendelbo, D. E. Akporiaye, A. Karlsson, M. Plassen and A. Olafsen, Combinatorial hydrothermal synthesis and characterisation of perovskites, *J. Eur. Ceram. Soc.*, 2006, **26**(6), 849–859.

40 A. Corma, M. J. Díaz-Cabãas, J. L. Jordá, C. Martínez and M. Moliner, High-throughput synthesis and catalytic properties of a molecular sieve with 18- and 10-member rings, *Nature*, 2006, **443**(7113), 842–845.

41 E. J. Roberts, S. E. Habas, L. Wang, D. A. Ruddy, E. A. White, F. G. Baddour, M. B. Griffin, J. A. Schaidle, N. Malmstadt and R. L. Brutchey, High-Throughput Continuous Flow Synthesis of Nickel Nanoparticles for the Catalytic Hydrodeoxygenation of Guaiacol, *ACS Sustainable Chem. Eng.*, 2017, **5**(1), 632–639.

42 J. He, K. Dettelbach, D. Salvatore, T. Li and C. Berlinguette, High-throughput synthesis of mixed-metal electrocatalysts for CO_2 reduction, *Angew. Chem.*, 2017, **56**, 6068–6072.

43 J. M. Caruthers, J. A. Lauterbach, K. T. Thomson, V. Venkatasubramanian, C. M. Snively, A. Bhan, S. Katare and G. Oskarsdottir, Catalyst design: Knowledge extraction from high-throughput experimentation, *J. Catal.*, 2003, **216**(1–2), 98–109.

44 W. F. Maier, K. Stowe and S. Sieg, Combinatorial and high-throughput materials science, *Angew. Chem., Int. Ed.*, 2007, **46**(32), 6016–6067.

45 S. Senkan, K. Krantz, S. Ozturk, V. Zengin and I. Onal, High-throughput testing of heterogeneous catalyst libraries using array microreactors and mass spectrometry, *Angew. Chem., Int. Ed.*, 1999, **38**(18), 2794–2799.

46 Q. He, J. Wu, S. Zhang, X. Fang, Z. Xing, C. Wei and X. Zhang, Rapid screening of gaseous catalysts in methane activation using ICP-QQQ-MS, *J. Anal. At. Spectrom.*, 2018, **33**(4), 563–568.

47 C. Hoffmann, H. W. Schmidt and F. Schüth, A Multipurpose Parallelized 49-Channel Reactor for the Screening of Catalysts: Methane Oxidation as the Example Reaction, *J. Catal.*, 2001, **198**(2), 348–354.

48 M. Kassem, M. Qun and S. M. Senkan, Chemical Structure of Fuel-Rich 1,2-$C_2H_4CI_2/CH_4$/02/Ar Flames: Effects of Micro-Probe Cooling on the Sampling of Flames of Chlorinated Hydrocarbons, *Combust. Sci. Technol.*, 1986, **67**(4–6), 147–157.

49 S. Senkan, High-throughput screening of solid-state catalyst libraries, *Nature*, 1998, **394**, 350–353.

50 M. Breysse, B. Claudel, L. Faure, M. Guenin, R. J. J. Williams and T. Wolkenstein, Chemiluminescence during the catalysis of carbon monoxide oxidation on a thoria surface, *J. Catal.*, 1976, **45**(2), 137–144.

51 X. Wang, N. Na, S. Zhang, Y. Wu and X. Zhang, Rapid screening of gold catalysts by chemiluminescence-based array imaging, *J. Am. Chem. Soc.*, 2007, **129**(19), 6062–6063.

52 S. Wang, Z. Yuan, L. Zhang, Y. Lin and C. Lu, Recent advances in cataluminescence-based optical sensing systems, *Analyst*, 2017, **142**(9), 1415–1428.

53 S. Wang, W. Shi and C. Lu, Chemisorbed Oxygen on the Surface of Catalyst-Improved Cataluminescence Selectivity, *Anal. Chem.*, 2016, **88**(9), 4987–4994.

54 N. Na, S. Zhang, S. Wang and X. Zhang, A catalytic nanomaterial-based optical chemo-sensor array, *J. Am. Chem. Soc.*, 2006, **128**(45), 14420–14421.

55 F. C. Moates, M. Somani, J. Annamalai, J. T. Richardson, D. Luss and R. C. Willson, Infrared Thermographic

Screening of Combinatorial Libraries of Heterogeneous Catalysts, *Ind. Eng. Chem. Res.*, 1996, **35**(12), 4801–4803.
56 J. Loskyll, K. Stoewe and W. F. Maier, Infrared thermography as a high-throughput tool in catalysis research, *ACS Comb. Sci.*, 2012, **14**(5), 295–303.
57 M. Krämer, M. Duisberg, K. Stöwe and W. F. Maier, Highly selective CO methanation catalysts for the purification of hydrogen-rich gas mixtures, *J. Catal.*, 2007, **251**(2), 410–422.
58 B. Weidenhof, M. Reiser, K. Stöwe, W. F. Maier, M. Kim, J. Azurdia, E. Gulari, E. Seker, A. Barks and R. M. Laine, High-throughput screening of nanoparticle catalysts made by flame spray pyrolysis as hydrocarbon/NO oxidation catalysts, *J. Am. Chem. Soc.*, 2009, **131**(26), 9207–9219.
59 S. Frost, S. Guérin, B. E. Hayden, J. P. Soulié and C. Vian, High-Throughput Synthesis and Characterization of Eu Doped $Ba_xSr_{2-x}SiO_4$ Thin Film Phosphors, *ACS Comb. Sci.*, 2018, **20**(7), 451–460.
60 J. Urschey, A. Kühnle and W. F. Maier, Combinatorial and conventional development of novel dehydrogenation catalysts, *Appl. Catal., A*, 2003, **252**(1), 91–106.
61 H. Su and E. S. Yeung, High-throughput screening of heterogeneous catalysts by laser-induced fluorescence imaging, *J. Am. Chem. Soc.*, 2000, **122**(30), 7422–7423.
62 H. Su, Y. Hou, R. S. Houk, G. L. Schrader and E. S. Yeung, Combinatorial screening of heterogeneous catalysts in selective oxidation of naphthalene by laser-induced fluorescence imaging, *Anal. Chem.*, 2001, **73**(18), 4434–4440.
63 R. A. Potyrailo, J. P. Lemmon and T. K. Leib, High-throughput screening of selectivity of melt polymerization catalysts using fluorescence spectroscopy and two-wavelength fluorescence imaging, *Anal. Chem.*, 2003, **75**(17), 4676–4681.
64 E. Sasmaz, K. Mingle and J. Lauterbach, High-throughput screening using Fourier-transform infrared imaging, *Engineering*, 2015, **1**(2), 234–242.
65 C. M. Snively, S. Katzenberger, G. Oskarsdottir and J. Lauterbach, Fourier-transform infrared imaging using a rapid-scan spectrometer, *Opt. Lett.*, 1999, **24**(24), 1841.
66 P. Kubanek, O. Busch, S. Thomson, H. W. Schmidt and F. Schüth, Imaging reflection IR spectroscopy as a tool to achieve higher integration for high-throughput experimentation in catalysis research, *J. Comb. Chem.*, 2004, **6**(3), 420–425.
67 G. Li, D. Hu, G. Xia, J. M. White and C. Zhang, High throughput operando studies using Fourier transform infrared imaging and Raman spectroscopy, *Rev. Sci. Instrum.*, 2008, **79**(7), 74101.
68 O. M. Busch, W. Brijoux, S. Thomson and F. Schüth, Spatially resolving infrared spectroscopy for parallelized characterization of acid sites of catalysts via pyridine sorption: Possibilities and limitations, *J. Catal.*, 2004, **222**(1), 174–179.
69 L. Takahashi and K. Takahashi, Visualizing Scientists' Cognitive Representation of Materials Data through the Application of Ontology, *J. Phys. Chem. Lett.*, 2019, **10**(23), 7482–7491.
70 A. J. Medford, M. R. Kunz, S. M. Ewing, T. Borders and R. Fushimi, Extracting Knowledge from Data through Catalysis Informatics, *ACS Catal.*, 2018, **8**(8), 7403–7429.
71 S. C. Sieg, C. Suh, T. Schmidt, M. Stukowski, K. Rajan and W. F. Maier, Principal component analysis of catalytic functions in the composition space of heterogeneous catalysts, *QSAR Comb. Sci.*, 2007, **26**(4), 527–535.
72 J. R. Monnier, W. Diao, S. Ma, M. T. Schaal and C. D. DiGiulio, An investigation on the role of Re as a promoter in Ag Cs Re/α-Al 2 O 3 high-selectivity, ethylene epoxidation catalysts, *J. Catal.*, 2014, **322**, 14–23.
73 V. Bukhtiyarov and A. Knop-gericke, Ethylene Epoxidation over Silver Catalysts, *Nanostructured Catalysts: Selective Oxidations*, 2011.
74 M. Huš and A. Hellman, Dipole effect on ethylene epoxidation: Influence of alkali metals and chlorine, *J. Catal.*, 2018, **363**, 18–25.
75 D. Ren, H. Xu, J. Li, J. Li and D. Cheng, Origin of enhanced ethylene oxide selectivity by Cs-promoted silver catalyst, *Mol. Catal.*, 2017, **441**, 92–99.
76 R. M. Lambert, F. J. Williams, R. L. Cropley and A. Palermo, Heterogeneous alkene epoxidation: past, present and future, *J. Mol. Catal. A: Chem.*, 2005, **228**, 27–33.
77 J. T. Jankowiak and M. A. Barteau, Ethylene epoxidation over silver and copper-silver bimetallic catalysts: I. Kinetics and selectivity, *J. Catal.*, 2005, **236**(2), 366–378.
78 A. Chongterdtoonskul, J. W. Schwank and S. Chavadej, Comparative study on the influence of second metals on Ag-loaded mesoporous SrTiO3 catalysts for ethylene oxide evolution, *J. Mol. Catal. A: Chem.*, 2013, **372**, 175–182.
79 J. W. Bae, E. J. Jang, B. I. Lee, J. S. Lee and K. H. Lee, Effects of tin on product distribution and catalyst stability in hydrodechlorination of CCl_4 over Pt-Sn/γ-Al_2O_3, *Ind. Eng. Chem. Res.*, 2007, **46**(6), 1721–1730.
80 J. C. Dellamorte, J. Lauterbach and M. A. Barteau, Palladium-silver bimetallic catalysts with improved activity and selectivity for ethylene epoxidation, *Appl. Catal., A*, 2011, **391**(1–2), 281–288.
81 R. Ren, Y. Lü, X. Pang and G. Wang, Metal catalyzed ethylene epoxidation: A comparative density functional theory study, *J. Nat. Gas Chem.*, 2011, **20**(3), 303–310.
82 E. A. Podgornov, I. P. Prosvirin and V. I. X. P. S. Bukhtiyarov, TPD and TPR studies of Cs-O complexes on silver: Their role in ethylene epoxidation, *J. Mol. Catal. A: Chem.*, 2000, **158**(1), 337–343.
83 J. C. Dellamorte, M. A. Barteau and J. Lauterbach, Opportunities for catalyst discovery and development: Integrating surface science and theory with high throughput methods, *Surf. Sci.*, 2009, **603**(10–12), 1770–1775.
84 S. Linic, J. Jankowiak and M. A. Barteau, Selectivity driven design of bimetallic ethylene epoxidation catalysts from first principles, *J. Catal.*, 2004, **224**(2), 489–493.
85 K. C. Waugh and M. Hague, The detailed kinetics and mechanism of ethylene epoxidation on an oxidised Ag/α-Al_2O_3 catalyst, *Catal. Today*, 2010, **157**(1–4), 44–48.

86 H. T. Chen, J. G. Chang, S. P. Ju and H. L. Chen, Ethylene epoxidation on a Au nanoparticle versus a Au(111) surface: A DFT study, *J. Phys. Chem. Lett.*, 2010, **1**(4), 739–742.

87 J. C. Dellamorte, J. Lauterbach and M. A. Barteau, Effect of preparation conditions on Ag catalysts for ethylene epoxidation, *Top. Catal.*, 2010, **53**(1–2), 13–18.

88 S. Rojluechai, S. Chavadej, J. W. Schwank and V. Meeyoo, Catalytic activity of ethylene oxidation over Au, Ag and Au-Ag catalysts: Support effect, *Catal. Commun.*, 2007, **8**(1), 57–64.

89 J. C. Dellamorte, J. Lauterbach and M. A. Barteau, Rhenium promotion of Ag and Cu–Ag bimetallic catalysts for ethylene epoxidation, *Catal. Today*, 2007, **120**(2), 182–185.

90 G. Ertl, H. Knozinger and J. Weitkamp, Preparation of Solid Catalysts, *Handbook of Heterogeneous Catalysis*, 1997, pp. 49–426.

91 D. S. Mannel, M. S. Ahmed, T. W. Root and S. S. Stahl, Discovery of multicomponent heterogeneous catalysts via admixture screening: PdBiTe catalysts for aerobic oxidative esterification of primary alcohols, *J. Am. Chem. Soc.*, 2017, **139**(4), 1690–1698.

92 B. A. Steinhoff, I. A. Guzei and S. S. Stahl, Mechanistic characterization of aerobic alcohol oxidation catalyzed by $Pd(OAc)_2$/pyridine including identification of the catalyst resting state and the origin of nonlinear [catalyst] dependence, *J. Am. Chem. Soc.*, 2004, **126**(36), 11268–11278.

93 B. A. Steinhoff and S. S. Stahl, Mechanism of $Pd(OAc)_2$/DMSO-catalyzed aerobic alcohol oxidation: Mass-transfer-limitation effects and catalyst decomposition pathways, *J. Am. Chem. Soc.*, 2006, **128**(13), 4348–4355.

94 M. Haruta, Catalysis of gold nanoparticles deposited on metal oxides, *CATTECH*, 2002, **6**(3), 102–115.

95 M. Haruta, S. Tsubota, T. Kobayashi, H. Kageyama, M. J. Genet and B. Delmon, Low-Temperature Oxidation of CO over Gold Supported on TiO_2, α-Fe_2O_3, and Co_3O_4, *J. Catal.*, 1993, **144**(1), 175–192.

96 J. Emmanuel, B. E. Hayden and J. Saleh-Subaie, The particle size dependence of CO oxidation on model planar titania supported gold catalysts measured by parallel thermographic imaging, *J. Catal.*, 2019, **369**, 175–180.

97 J. G. Wang and B. Hammer, Role of Au^+ in supporting and activating Au_7 on TiO_2(110), *Phys. Rev. Lett.*, 2006, **97**(13), 1–4.

98 M. Kotobuki, R. Leppelt, D. A. Hansgen, D. Widmann and R. J. Behm, Reactive oxygen on a Au/TiO_2 supported catalyst, *J. Catal.*, 2009, **264**, 67–76.

99 D. Li, S. Chen, R. You, Y. Liu, M. Yang, T. Cao, K. Qian, Z. Zhang, J. Tian and W. Huang, Titania-morphology-dependent dual-perimeter-sites catalysis by Au/TiO_2 catalysts in low-temperature CO oxidation, *J. Catal.*, 2018, **368**, 163–171.

100 Z. Y. Hou, Q. Dai, X. Q. Wu and G. T. Chen, Artificial neural network aided design of catalyst for propane ammoxidation, *Appl. Catal., A*, 1997, **161**(1–2), 183–190.

101 O. I. Abiodun, A. Jantan, A. E. Omolara, K. V. Dada, N. A. E. Mohamed and H. Arshad, *State-of-the-art in artificial neural network applications: a survey*, Elsevier Ltd, Heliyon, 2018, vol. 4.

102 L. K. Hansen and P. Salamon, Neural Network Ensembles, *IEEE Trans. Pattern Anal. Mach. Intell.*, 1990, **12**(10), 993–1001.

103 G. G. Towell and J. W. Shavlik, Extracting Refined Rules from Knowledge-Based Neural Networks, *Mach. Learn.*, 1993, **13**(1), 71–101.

104 M. E. Günay and R. Yildirim, Modeling preferential CO oxidation over promoted Au/Al_2O_3 catalysts using decision trees and modular neural networks, *Chem. Eng. Res. Des.*, 2013, **91**(5), 874–882.

105 I. A. Basheer and M. Hajmeer, Artificial neural networks: Fundamentals, computing, design, and application, *J. Microbiol. Methods*, 2000, **43**(1), 3–31.

106 A. Jain, S. P. Ong, G. Hautier, W. Chen, W. D. Richards, S. Dacek, S. Cholia, D. Gunter, D. Skinner, G. Ceder and K. A. Persson, Commentary: The materials project: A materials genome approach to accelerating materials innovation, *APL Mater.*, 2013, **1**, 011002.

107 K. Kim, L. Ward, J. He, A. Krishna, A. Agrawal and C. Wolverton, Machine-learning-accelerated high-throughput materials screening: Discovery of novel quaternary Heusler compounds, *Phys. Rev. Mater.*, 2018, **2**(12), 1–9.

108 P. Raccuglia, K. C. Elbert, P. D. F. Adler, C. Falk, M. B. Wenny, A. Mollo, M. Zeller, S. A. Friedler, J. Schrier and A. J. Norquist, Machine-learning-assisted materials discovery using failed experiments, *Nature*, 2016, **533**(7601), 73–76.

109 L. M. Ghiringhelli, J. Vybiral, S. V. Levchenko, C. Draxl and M. Scheffler, Big data of materials science: Critical role of the descriptor, *Phys. Rev. Lett.*, 2015, **114**(10), 1–5.

110 A. J. Chowdhury, W. Yang, E. Walker, O. Mamun, A. Heyden and G. A. Terejanu, Prediction of Adsorption Energies for Chemical Species on Metal Catalyst Surfaces Using Machine Learning, *J. Phys. Chem. C*, 2018, **122**(49), 28142–28150.

111 L. Breiman, Random forests, *Mach. Learn.*, 2001, **45**(1), 5–32.

112 C. Cortes and V. Vapnik, Support-Vector Networks, *Mach. Learn.*, 1995, **20**(3), 273–297.

113 C. Hans, Bayesian lasso regression, *Biometrika*, 2009, **96**(4), 835–845.

114 D. P. Tabor, L. M. Roch, S. K. Saikin, C. Kreisbeck, D. Sheberla, J. H. Montoya, S. Dwaraknath, M. Aykol, C. Ortiz, H. Tribukait, C. Amador-Bedolla, C. J. Brabec, B. Maruyama, K. A. Persson and A. Aspuru-Guzik, Accelerating the discovery of materials for clean energy in the era of smart automation, *Nat. Rev. Mater.*, 2018, **3**(5), 5–20.

115 D. H. Wolpert and W. G. Macready, No free lunch theorems for optimization, *IEEE Trans. Evol. Comput.*, 1997, **1**(1), 67–82.

116 D. H. Wolpert and W. G. Macready, Coevolutionary free lunches, *IEEE Trans. Evol. Comput.*, 2005, **9**(6), 721–735.

117 U. Zavyalova, M. Holena, R. Schlögl and M. Baerns, Statistical analysis of past catalytic data on oxidative methane

coupling for new insights into the composition of high-performance catalysts, *ChemCatChem*, 2011, **3**(12), 1935–1947.
118 V. Stanev, C. Oses, A. G. Kusne, E. Rodriguez, J. Paglione, S. Curtarolo and I. Takeuchi, Machine learning modeling of superconducting critical temperature, *npj Comput. Mater.*, 2018, **4**(1), 1–14.
119 M. R. Munafò, B. A. Nosek, D. V. M. Bishop, K. S. Button, C. D. Chambers, N. Percie Du Sert, U. Simonsohn, E. J. Wagenmakers, J. J. Ware and J. P. A. Ioannidis, A manifesto for reproducible science, *Nature Human Behaviour*, Macmillan Publishers Limited, 2017, vol. 1, pp. 1–9.
120 R. D. Peng, Reproducible Research in Pattern Recognition, *RRPR: International Workshop on Reproducible Reserach in Pattern Recognition*, 2017, pp. 1226–8.
121 T. N. Nguyen, T. T. P. Nhat, K. Takimoto, A. Thakur, S. Nishimura, J. Ohyama, I. Miyazato, L. Takahashi, J. Fujima, K. Takahashi and T. Taniike, High-Throughput Experimentation and Catalyst Informatics for Oxidative Coupling of Methane, *ACS Catal.*, 2020, **10**(2), 921–932.
122 B. Meredig, A. Agrawal, S. Kirklin, J. E. Saal, J. W. Doak, A. Thompson, K. Zhang, A. Choudhary and C. Wolverton, Combinatorial screening for new materials in unconstrained composition space with machine learning, *Phys. Rev. B: Condens. Matter Mater. Phys.*, 2014, **89**(9), 1–7.
123 D. Farrusseng, C. Klanner, L. Baumes, M. Lengliz, C. Mirodatos and F. Schüth, Design of discovery libraries for solids based on QSAR models, *QSAR and Combinatorial Science*, 2005, pp. 78–93.
124 D. Farrusseng, F. Clerc, C. Mirodatos and R. Rakotomalala, Virtual screening of materials using neuro-genetic approach: Concepts and implementation, *Comput. Mater. Sci.*, 2009, **45**(1), 52–59.
125 J. Hill, A. Mannodi-Kanakkithodi, R. Ramprasad and B. Meredig, Materials data infrastructure and materials informatics, *Computational Materials System Design*, 2017, pp. 193–225.
126 E. J. Kluender, J. L. Hedrick, K. A. Brown, R. Rao, B. Meckes, J. S. Du, L. M. Moreau, B. Maruyama and C. A. Mirkin, Catalyst discovery through mega libraries of nanomaterials, *Proc. Natl. Acad. Sci. U. S. A.*, 2019, **116**(1), 40–45.
127 Z. Li, S. Wang and H. Xin, Toward artificial intelligence in catalysis, *Nat. Catal.*, 2018, **1**(9), 641–642.
128 J. R. Kitchin, Machine learning in catalysis, *Nat. Catal.*, 2018, **1**(4), 230–232.
129 E. Walker, S. C. Ammal, G. A. Terejanu and A. Heyden, Uncertainty Quantification Framework Applied to the Water-Gas Shift Reaction over Pt-Based Catalysts, *J. Phys. Chem. C*, 2016, **120**(19), 10328–10339.
130 Z. W. Ulissi, A. J. Medford, T. Bligaard and J. K. Nørskov, To address surface reaction network complexity using scaling relations machine learning and DFT calculations, *Nat. Commun.*, 2017, **8**, 1–7.
131 B. R. Goldsmith, J. Esterhuizen, J.-X. Liu, C. J. Bartel and C. Sutton, Machine learning for heterogeneous catalyst design and discovery, *AIChE J.*, 2018, **64**(7), 2311–2323.
132 S. Kito, T. Hattori and Y. Murakami, Estimation of catalytic performance by neural network—product distribution in oxidative dehydrogenation of ethylbenzene, *Appl. Catal., A*, 1994, **114**(2), L173–L178.
133 M. Sasaki, H. Hamada, Y. Kintaichi and T. Ito, Application of a neural network to the analysis of catalytic reactions Analysis of NO decomposition over Cu/ZSM-5 zeolite, *Appl. Catal., A*, 1995, **132**(2), 261–270.
134 D. Wolf, O. V. Buyevskaya and M. Baerns, Evolutionary approach in the combinatorial selection and optimization of catalytic materials, *Appl. Catal., A*, 2000, **200**(1), 63–77.
135 M. Holeňa and M. Baerns, Feedforward neural networks in catalysis: A tool for the approximation of the dependency of yield on catalyst composition, and for knowledge extraction, *Catal. Today*, 2003, **81**(3), 485–494.
136 U. Rodemerck, M. Baerns, M. Holena and D. Wolf, Application of a genetic algorithm and a neural network for the discovery and optimization of new solid catalytic materials, *Appl. Surf. Sci.*, 2004, **223**(1–3), 168–174.
137 D. Lukyanov, N. Gnep and M. Guisnet, Kinetic modeling of propane aromatization reaction over HZSM-5 and GaHZSM-5, *Ind. Eng. Chem. Res.*, 1995, **34**(2), 516–523.
138 A. Corma, J. M. Serra, E. Argente, V. Botti and S. Valero, Application of artificial neural networks to combinatorial catalysis: Modeling and predicting ODHE catalysts, *ChemPhysChem*, 2002, **3**(11), 939–945.
139 L. Baumes, D. Farrusseng, M. Lengliz and C. Mirodatos, Using artificial neural networks to boost high-throughput discovery in heterogeneous catalysis, *QSAR Comb. Sci.*, 2004, **23**(9), 767–778.
140 A. Corma, J. M. Serra, P. Serna, S. Valero, E. Argente and V. Botti, Optimisation of olefin epoxidation catalysts with the application of high-throughput and genetic algorithms assisted by artificial neural networks (softcomputing techniques), *J. Catal.*, 2005, **229**(2), 513–524.
141 J. M. Serra, A. Corma, S. Valero, E. Argente and V. Botti, Soft computing techniques applied to combinatorial catalysis: A new approach for the discovery and optimization of catalytic materials, *QSAR Comb. Sci.*, 2007, **26**(1), 11–26.
142 A. Corma, J. M. Serra, P. Serna and M. Moliner, Integrating high-throughput characterization into combinatorial heterogeneous catalysis: Unsupervised construction of quantitative structure/property relationship models, *J. Catal.*, 2005, **232**(2), 335–341.
143 J. M. Serra, A. Chica and A. Corma, Development of a low temperature light paraffin isomerization catalysts with improved resistance to water and sulphur by combinatorial methods, *Appl. Catal., A*, 2003, **239**(1–2), 35–42.
144 T. Williams, K. McCullough and J. A. Lauterbach, Enabling Catalyst Discovery through Machine Learning and High-Throughput Experimentation, *Chem. Mater.*, 2020, **32**(1), 157–165.
145 W. Pyrz, R. Vijay, J. Binz, J. Lauterbach and D. J. Buttrey, Characterization of K-promoted Ru catalysts for ammonia decomposition discovered using high-throughput experimentation, *Top. Catal.*, 2008, **50**(1–4), 180–191.

146 C. M. Snively, G. Oskarsdottir and J. Lauterbach, Parallel analysis of the reaction products from combinatorial catalyst libraries, *Angew. Chem., Int. Ed.*, 2001, **40**(16), 3028–3030.

147 A. K. Hill and L. Torrente-Murciano, Low temperature H2 production from ammonia using ruthenium-based catalysts: Synergetic effect of promoter and support, *Appl. Catal., B*, 2015, **172–173**, 129–135.

148 A. J. Medford, A. Vojvodic, J. S. Hummelshøj, J. Voss, F. Abild-Pedersen, F. Studt, T. Bligaard, A. Nilsson and J. K. Nørskov, From the Sabatier principle to a predictive theory of transition-metal heterogeneous catalysis, *J. Catal.*, 2015, **328**, 36–42.

149 X. Ma, Z. Li, L. E. K. Achenie and H. Xin, Machine-Learning-Augmented Chemisorption Model for CO_2 Electroreduction Catalyst Screening, *J. Phys. Chem. Lett.*, 2015, **6**(18), 3528–3533.

150 I. Takigawa, K. I. Shimizu, K. Tsuda and S. Takakusagi, Machine-learning prediction of the d-band center for metals and bimetals, *RSC Adv.*, 2016, **6**(58), 52587–52595.

151 Z. Li, S. Wang, W. S. Chin, L. E. Achenie and H. Xin, High-throughput screening of bimetallic catalysts enabled by machine learning, *J. Mater. Chem. A*, 2017, **5**(46), 24131–24138.

152 D. C. Montgomery, *Design and analysis of experiments*, Wiley, New York, 1984.

153 S. R. Fisher, *The design of experiments*, Hafner Publishing Company, 9th edn, 1971.

154 T. Mueller, A. Kusne and R. Ramprasad, Machine learning in materials science: Recent progress and emerging applications, *Rev. Comput. Chem.*, 2016, **29**, 186–273.

155 B. Shahriari, K. Swersky, Z. Wang, R. P. Adams and N. De Freitas, Taking the human out of the loop: A review of Bayesian optimization, *Proceedings of the IEEE*, IEEE, 2016, pp. 148–75.

156 A. D. Bull, Convergence rates of efficient global optimization algorithms, *J. Mach. Learn. Res.*, 2011, 2879–2904.

157 N. Srinivas, A. Krause, S. M. Kakade and M. W. Seeger, Information-theoretic regret bounds for Gaussian process optimization in the bandit setting, *IEEE Trans. Inf. Theory*, 2012, **58**(5), 3250–3265.

158 T. Theckel Joy, S. Rana, S. Gupta and S. Venkatesh, A flexible transfer learning framework for Bayesian optimization with convergence guarantee, *Expert Syst. Appl.*, 2019, **115**, 656–672.

159 P. Jamshidi, M. Velez, C. Kästner, N. Siegmund and P. Kawthekar, Transfer Learning for Improving Model Predictions in Highly Configurable Software, in Proceedings – 2017 IEEE/ACM 12th International Symposium on Software Engineering for Adaptive and Self-Managing Systems, SEAMS 2017, 2017, pp. 31–41.

160 J. Song, Y. Chen and Y. Yue, A general framework for multi-fidelity Bayesian optimization with Gaussian processes, in The 22nd International Conference on Artificial Intelligence and Statistics, 2019, pp. 3158–3167.

161 J. Wu, S. Toscano-Palmerin, P. Fraizer and A. Gordan, Practical multi-fidelity bayesian optimization for hyperparameter tuning, in 35th Conference on Uncertainty in Artificial Intelligence, 2019.

162 K. Kandasamy, G. Dasarathy, J. Schneider and B. Poczos, The multi-fidelity multi-armed bandit, in Proceedings of the 30th International Conference on Neural Information Processing Systems, 2016, pp. 1785–1793.

163 R. Sen, K. Kandasamy and S. Shakkottai, Multi-fidelity black-box optimization with hierarchical partitions, in International Conference on Machine Learning, 2018, pp. 4538–4537.

164 J. Pearl, *Causality*, Cambridge University Press, 2009.

165 P. Jamshidi, N. Siegmund, M. Velez, C. Kastner, A. Patel and Y. Agarwal, Transfer learning for performance modeling of configurable systems: An exploratory analysis, in ASE 2017 – Proceedings of the 32nd IEEE/ACM International Conference on Automated Software Engineering, 2017, pp. 497–508.

166 P. Jamshidi, M. Velez, C. Kästner and N. Siegmund, Learning to sample: exploiting similarities across environments to learn performance models for configurable systems, in ESEC/FSE 2018 – Proceedings of the 2018 26th ACM Joint Meeting on European Software Engineering Conference and Symposium on the Foundations of Software Engineering, 2018, pp. 71–82.

167 M. Long, Y. Cao, J. Wang and M. Jordan, Learning transferable features with deep adaptation networks, in Proc of Int'l Conference on Machine Learning (ICML), 2015, pp. 97–105.

168 J. Yosinski, J. Clune, Y. Bengio and H. Lipson, How transferable are features in deep neural networks? in Proc of 12th USENIX conference on Operating Systems Design and Implementation (OSDI), 2014, pp. 3320–3328.

169 M. A. Javidian, P. Jamshidi and M. Valtorta, Transfer Learning for Performance Modeling of Configurable Systems: A Causal Analysis, 2019, arXiv:1902.10119.

170 M. T. Ribeiro, S. Singh and C. Guestrin, "Why should i trust you?" Explaining the predictions of any classifier, in Proceedings of the ACM SIGKDD International Conference on Knowledge Discovery and Data Mining, 2016, pp. 1135–1144.

171 G. Marcus, Deep learning: a critical appraisal, 2018, arXiv:1801.00631, pp. 1–24.

172 J. Y. Halpern and J. Pearl, Causes and explanations: A structural-model approach. Part I: Causes, *Br. J. Philos. Sci.*, 2005, **56**(4), 843–887.

173 J. Peter, D. Janzing and B. Schölkopf, *Elements of casual inference: foundations of learning algorithms*, MIT Press, 2017.

174 J. Pearl, Causality, *IIE Trans.*, 2002, **34**(6), 583–589.

175 A. Subbaswamy and S. Saria, Counterfactual Normalization: Proactively Addressing Dataset Shift and Improving Reliability Using Causal Mechanisms, *Proceedings of the 34th Conference on Uncertainty in Artificial Intelligence (UAI)*, 2018.

176 J. Pearl and D. Mackenzie, *The Book of Why: The New Science of Cause and Effect, Basic Books*, 1st edn, 2019.

177 J. Pearl, The seven tools of causal inference, with reflections on machine learning, *Commun. ACM*, 2019, **62**(3), 54–60.

178 M. B. L. Arjovsky, I. Gulrajani and D. Lopez-Paz, Invariant risk minimization, *Statistics*, 2019, 5.
179 B. Schölkopf, D. Janzing, J. Peters, E. Sgouritsa, K. Zhang and J. Mooij, On causal and anticausal learning, *Proceedings of the 29th International Conference on International Conference on Machine Learning*, 2012.
180 D. Xue, P. V. Balachandran, J. Hogden, J. Theiler, D. Xue and T. Lookman, Accelerated search for materials with targeted properties by adaptive design, *Nat. Commun.*, 2016, **7**(1), 1–9.
181 C. Li, D. Rubín De Celis Leal, S. Rana, S. Gupta, A. Sutti, S. Greenhill, T. Slezak, M. Height and S. Venkatesh, Rapid Bayesian optimisation for synthesis of short polymer fiber materials, *Sci. Rep.*, 2017, **7**(1), 1–10.
182 D. Krishnamurthy, H. Weiland, A. Barati Farimani, E. Antono, J. Green and V. Viswanathan, Machine Learning Based Approaches to Accelerate Energy Materials Discovery and Optimization, *ACS Energy Lett.*, 2019, **4**(1), 187–191.
183 R. Gómez-Bombarelli, J. N. Wei, D. Duvenaud, J. M. Hernández-Lobato, B. Sánchez-Lengeling, D. Sheberla, J. Aguilera-Iparraguirre, T. D. Hirzel, R. P. Adams and A. Aspuru-Guzik, Automatic Chemical Design Using a Data-Driven Continuous Representation of Molecules, *ACS Cent. Sci.*, 2018, **4**(2), 268–276.
184 R.-R. Griffiths and J. M. Hernández-Lobato, Constrained Bayesian Optimization for Automatic Chemical Design, 2017, arXiv:1709.05501, pp. 1–17.
185 F. Häse, L. M. Roch, C. Kreisbeck and A. Aspuru-Guzik, Phoenics: A Bayesian Optimizer for Chemistry, *ACS Cent. Sci.*, 2018, **4**(9), 1134–1145.
186 K. Korovina, S. Xu, K. Kandasamy, W. Neiswanger, B. Poczos, J. Schneider and E. P. Xing, ChemBO: Bayesian Optimization of Small Organic Molecules with Synthesizable Recommendations, 2019, arXiv:1908.01425, pp. 1–19.
187 T. Lookman, P. Balachandran, D. Xue and R. Yuan, Active learning in materials science with emphasis on adaptive sampling using uncertainties for targeted design, *npj Comput. Mater.*, 2019, **5**(1), 1–17.
188 J. Dean, R. M. Corrado, K. Chen, M. Devin, M. Mao, M. Ranzato, A. Senior, P. Tucker, K. Yang, Q. Le and A. Ng, Large scale distributed deep networks, *Advances in neural information processing systems*, 2012.

